An assessment of remotely sensed surface and root zone soil moisture through active and passive sensors in northeast Asia

Eunsang Cho [a], Minha Choi [b,*], Wolfgang Wagner [c]

[a] Department of Civil and Environmental Engineering, Hanyang University, Seoul 133-791, Republic of Korea

[b] Water Resources and Remote Sensing Laboratory, Department of Water Resources, Graduate School of Water Resources, Sungkyunkwan University, Suwon 440-746, Republic of Korea

[c] Department of Geodesy and Geo-information, Vienna University of Technology, Vienna, Austria

eunsangcho@hanyang.ac.kr

mhchoi@skku.edu

wolfgang.wagner@geo.tuwien.ac.at

Revision submitted to Remote Sensing of Environment

December 16, 2014

*Corresponding author

Department of Water Resources, Graduate School of Water Resources,

Sungkyunkwan University, Suwon 440-746, Korea

Tel: 82-31-290-7527

Fax: 82-31-290-7549

Email: mhchoi@skku.edu

Abstract

Active and passive microwave remote sensing techniques provide an effective way to observe soil moisture contents. We validated Advanced Scatterometer (ASCAT) and Advanced Microwave Scanning Radiometer – Earth Observing System (AMSR-E) sensor products using estimations from nine different stations located in the Korean peninsula, in northeast Asia from May 1 to September 30, 2010. The results of the surface soil moisture (SSM) products showed reasonable agreement with the average correlation coefficient (R) values of 0.39, 0.42, and 0.53 for the National Snow and Ice Data Centre (NSIDC), Vrije Universiteit Amsterdam – National Aeronautics and Space Administration (VUA-NASA) AMSR-E, and ASCAT SSM datasets, respectively. The root zone soil moisture (RZSM) products, derived using the NSIDC soil water index (SWI), the United States Department of Agriculture (USDA) AMSR-E, and the ASCAT SWI datasets showed relatively high R values of 0.47, 0.72, and 0.75, respectively, with *in situ* soil moisture at a depth of 20 cm. In particular, AMSR-E USDA RZSM data show best agreements with in-situ data at 20 cm, among the four depths (10, 20, 30, and 50 cm). In this study, the ASCAT SSM and SWI were rescaled based on the porosity and the effective saturation according to soil texture. Renormalized soil moisture products using three renormalization methods: the linear regression correction (REG), average-standard deviation ($\mu-\sigma$), and cumulative distribution function (CDF) provided an improvement in biases and RMSEs, with SSM (SWI) RMSEs of 0.04 (0.02), 0.05 (0.03), and 0.05 (0.03) m^3/m^3 for REG, $\mu-\sigma$, and CDF matching, respectively. A Taylor diagram was used to assess the accuracy of four satellite soil moisture products with *in situ* data on a plot. Based on these results, ASCAT soil moisture products were potentially proven to be more appropriate than AMSR-E products in northeast Asia. Remotely sensed soil moisture datasets from passive (AMSR-E) and active (ASCAT) sensors are beneficial to

operational hydrological investigations and water management activities.

Keywords

Remotely sensed soil moisture, AMSR-E, ASCAT, root zone soil moisture, validation

1. Introduction

Soil moisture (SM) is an essential variable in the hydrological cycle, although it occupies only 0.15% of the liquid freshwater on the earth (Western et al., 2002). It plays an important role in hydrological and meteorological activity, together with weather, climate predictions, water resources and irrigational management, as well as hazard analysis. Since 2010, it has been considered an essential climate variable (ECV) by the World Meteorological Organization (WMO, 2010). SM has strong spatio-temporal variability, caused by the heterogeneity of soil properties, land cover, vegetation, and topography, as well as climate conditions (Brocca et al., 2007; Cho & Choi, 2014; Choi & Jacobs, 2007; Famiglietti et al., 2008; Jacobs et al., 2004; Schmugge et al., 2002; Sur et al., 2013). At present, ground-based SM measurement methods, such as neutron probes, time-domain reflectometry (TDR), and frequency-domain reflectometry (FDR), provide accurate moisture contents estimation at point scale. With the growing need for large-scale observations of the spatial patterns of soil moisture, there has been an increased focus on the use of remote sensing techniques (Schmugge et al., 2002; Jackson et al., 2010).

Remote sensing instruments, including aircraft or satellites with active and passive microwave sensors, have facilitated the measurement of the surface soil moisture for large areas (Njoku & Entekhabi, 1996), including the spatial and temporal characterization of surface fields (Njoku et al., 2002). Microwave sensors can observe SSM, as the effects of moisture change on the emissivity or backscattering of the surface (Njoku et al., 2003). In particular, satellites using passive or active microwave sensors have been demonstrated to provide useful retrievals of near-surface soil moisture variations, at both regional and global scales (Gruhier et al., 2010; Jackson et al., 2002; Wagner et al., 1999b). The inter-comparison and validation of remotely sensed soil moisture products is a challenging task, because of the differences between satellite and ground based measurements at both spatial and temporal scales (Jackson et al., 1996, 2010).

Since the Scanning Multichannel Microwave Radiometer (SMMR), the first passive microwave sensor on a satellite, was in operation from 1978 to 1987, there has been a series of passive microwave sensors capable of providing soil moisture data. Most notable are the Tropical Rainfall Measuring Mission (TRMM) Microwave Imager (TMI; 1997-present), the Advanced Microwave Scanning Radiometer for the Earth Observing System (AMSR-E; 2002-2011), WindSat (2003-present), and the Soil Moisture and Ocean Salinity Mission (SMOS; 2009-present). The most recent instrument is the Advanced Microwave Scanning Radiometer 2 (AMSR2), which was launched by the Japan Aerospace Exploration Agency (JAXA) on the Global Change Observation Mission – Water (GCOM–W) in May 2012.

Active microwave instruments, such as the SCATterometer (SCAT) onboard European Remote Sensing (ERS-1 and ERS-2; 1991-2000, 1995-2011), and Advanced SCATterometer (ASCAT; 2007-present) onboard the Meteorological Operational satellite programme–A (MetOp-A), have carried out SSM measurement (Wagner et al., 1999b, 2013). Recently (September 2012), MetOp-B was developed as a joint undertaking between the European Space Agency (ESA), and the European Organization for the Exploitation of Meteorological Satellites (EUMETSAT). The World Meteorological Organization (WMO) has also increasingly recognized the importance of the use of earth observation satellites for soil moisture monitoring (WMO, 2013). Furthermore, the Soil Moisture Active and Passive (SMAP) launch, headed by the NASA, is planned for January 2015. The SMAP measurement approach uses two microwave instruments (an L-band synthetic aperture radar and an L-band radiometer), integrating these data in order to make high resolution (9-km) and high-accuracy measurements. This mission will provide global soil moisture measurements present at the

Earth's land surfaces and, in particular, will differentiate frozen from thawed land surfaces (Entekhabi et al., 2010a). Moreover, MetOp-C, the third and final satellite from the MetOp mission, will be launched in 2016, following MetOp-B, in order to provide continuous measurements of high-quality data, monitoring long-term weather and climate conditions until at least 2020. GCOM-W2, the 2nd flight unit of the GCOM-W program, is also expected to contribute to the monitoring of hydrological variables in 2016 (available online at http://www.wmo-sat.info/oscar/satellites). These continual satellite launches for the purpose of soil moisture observations will enable researchers to accelerate the development of remote sensing techniques.

Several studies demonstrated that blending observations taken from different satellite sensors were known as a promising approach in various fields (Liu et al., 2012; Yilmaz et al., 2012). Various researches using satellite soil moisture data have also consistently progressed in terms of applications, such as drought (Bolten et al., 2010; Zhang and Jia, 2013), runoff modeling (Brocca et al., 2010b, 2012), and flood forecasting (Bindlish et al., 2009). Recent validation studies have been conducted for satellite SSM retrievals (AMSR-E, SMOS, and ASCAT) comparing with *in situ* measurements for Europe, the United States and Australia (Albergel et al., 2012; Brocca et al., 2011; Su et al., 2013; Gruhier et al., 2010; Parinussa et al., 2013; Parrens et al., 2012). A few validation studies of the remotely sensed RZSM also have been performed (Albergel et al., 2008; Brocca et al., 2010a; Paulik et al., 2014).

In the current study, we evaluate the remotely sensed SSM and RZSM data, derived from active (ASCAT) and passive (AMSR-E) microwave sensors, by comparing it with ground based soil moisture measurements (10, 20, 30, and 50 cm) in northeast Asia. The three kinds of AMSR-E soil moisture retrievals were used for validation and inter-comparison: 1) NSIDC AMSR-E Level 3 SSM retrievals from the National Snow and Ice Data Centre (NSIDC), 2)

VUA-NASA AMSR-E developed by the Vrije Universiteit Amsterdam (VUA) with the National Aeronautics and Space Administration (NASA), and 3) USDA AMSR-E RZSM data using VUA-NASA SSM products. Moreover, ASCAT Level 3 SSM and SWI derived by the Vienna University of Technology (TU-Wien) were used. Unfortunately, the SMOS satellite data could not be used in this study, because of unavailability of the soil moisture data for northeast Asia due to Radio Frequency Interference (RFI) (Kerr et al., 2012; Leroux et al., 2013).

The main purpose of this study was to assess the accuracy of AMSR-E and ASCAT satellite-based SSM and RZSM products, and to determine which sensor was in better agreement with the ground based soil moisture patterns in northeast Asia. In particular, the satellite soil moisture products were systematically compared with *in situ* observations from nine different sites located in the Korean peninsula from May 1 to September 30, 2010. This research will be helpful to determine the accuracy of remotely sensed SSM and RZSM retrieval, as well as the expansion of various applications, such as drought monitoring, flood forecasting, and hydrological modeling.

2. Description of the study area and dataset

2.1. Ground Soil Moisture Measurement in the study area

Ground soil moisture observations are routinely used to evaluate remotely sensed SSM and RZSM. In the Korean peninsula, located in the middle (34-39°N and 126-130°E) of northeast Asia, ground soil moisture data were periodically collected at four different depths (10, 20, 30, and 50 cm), approximately over twenty sites installed by the Korea Meteorological Administration (KMA). On the basis of data quality and availability, eight sites, Suwon, Seosan, Jeonju, Cheorwon, Chuncheon, Andong, Cheongju, and Jinju, were selected for this validation study. We also selected an additional site, Seolmalcheon (SMC), operated by the Hydrological Survey Center (HSC), for using the ground soil moisture (10 cm) measurements (Fig. 1). Table 1 shows the main characteristics of each site: location (latitude, longitude and elevation), climate (mean annual rainfall, temperature and relative humidity), and physical characteristics (soil texture and land use). The climate is humid, and the annual rainfall ranges from 1074 to 2014 mm in the northern Korean peninsula. The heaviest rainfall usually occurs in summer, due to the East Asian monsoon (Kim et al., 2002; KMA, 2006). Most of the soil types are sandy loam and loam, and the land uses are urban, cropland, and mixed forest. In this study, the ground measured soil moisture data were collected by Frequency Domain Reflectometry (FDR), on an hourly basis. FDR sensor sends an electromagnetic wave along its probes, and measures the frequency of the reflected wave, which varies with the soil water content. Compared to Time Domain Reflectometry (TDR), FDR has several advantages. FDR is economical and requires lower electric power consumption and it enables users to continuously monitor soil moisture at several remote locations using automated data loggers (Veldkamp & O'Brien, 2000).

2.2. Advanced Microwave Scanning Radiometer - Earth Observing System (AMSR-E)

The AMSR-E instrument on board the Aqua satellite provided global microwave measurements using different bands (56 km for the C band, 38 km for the X band, and 12 km for the Ka band) from May 2002 to October 2011, with daily ascending (13:30, equatorial local crossing time) and descending (01:30, equatorial local crossing time) overpasses, over a swath width of 1445 km (Njoku et al., 2003, Njoku, 2010). We used different types of AMSR-E soil moisture products (Table 2): 1. NSIDC's X-band based SSM and RZSM products (Njoku et al., 2003), 2. VUA-NASA's C- and X-band based SSM products (Owe et al., 2008), and 3. USDA's C-band based RZSM products (Bolten et al., 2010; Bolten & Crow, 2012).

The NSIDC soil moisture retrieval algorithm is based on an iterative multichannel inversion procedure to compare the observed brightness temperatures, and the computed brightness temperatures. It is mainly affected by the volumetric water content of the soil, vegetation water content, and soil temperatures. For detailed descriptions of the algorithm, readers referred to Njoku et al. (2003). In response to RFI in the C-band AMSR–E data across much of North America and East Asia, the current version of NSIDC AMSR-E soil moisture was applied only to the X-band (Njoku et al., 2005; Draper et al., 2009). The VUA-NASA soil moisture products were retrieved using the Land Parameter Retrieval Model (LPRM). The LPRM is based on a radiative transfer model that looks for geophysical variables (SSM, vegetation water content, and soil/canopy temperature) to the brightness temperatures (T_b). It uses the dual polarized channel (either C-band 6.9 or X-band 10.6 GHz) for the retrieval of both SSM, and vegetation water content (VWC) (Owe et al., 2001, 2008). The vegetation optical depth is parameterized as a function of the microwave polarization difference index (MPDI):

$$MPDI = (T_{\mathrm{b(V)}} - T_{\mathrm{b(H)}}) / (T_{\mathrm{b(V)}} + T_{\mathrm{b(H)}}) \qquad (1)$$

where $T_{\mathrm{b(V)}}$ and $T_{\mathrm{b(H)}}$ are the vertical and horizontal brightness temperatures, respectively. For frequencies less than 10 GHz, the MPDI has relevance to the canopy and soil emission, and the soil dielectric properties. The soil emissivity is affected by soil moisture, by the effect of moisture on the soil dielectric constant (Meesters et al., 2005; Owe et al., 2008; de Jeu et al., 2014). We used an updated version of the AMSR-E soil moisture product derived by the VUA in collaboration with NASA.

The USDA RZSM data was derived by the assimilation of Land Parameter Retrieval Model

(LPRM) SSM retrievals (C-band, descending time), into the 2-Layer Palmer Water Balance Model (Bolten et al., 2010; Bolten & Crow, 2012). This data were downloaded from ftp://hydro1.sci.gsfc.nasa.gov/data/s4pa/WAOB/LPRM_AMSRE_D_RZSM3.001/. We extracted the Level 3 soil moisture values directly from the AMSR-E L3 Daily Land data files. The ground based soil moisture data were extracted at the Aqua satellite overpass time.

2.3. Advanced Scatterometer (ASCAT)

ASCAT is a real-aperture radar sensor measuring radar backscatter at C-band in VV polarization, with a radiometric accuracy better than 0.3 dB (Verspeek et al., 2010). It has a sun-synchronous orbit at 817 km, with equator crossing at 21:30 and 09:30. Measurements occur on both sides of the sub satellite track; therefore, two 550 km wide swaths of data are produced, with a spatial resolution of 25 km, resampled to a 12.5 km grid. Because ASCAT operates continuously, more than twice of the European Remote-sensing Satellite (ERS) scatterometer provided coverage (Bartalis et al., 2007). The C-band backscatter measurements are converted to soil moisture estimates, by applying the Technische Universität (TU) Wien soil moisture retrieval algorithm (Wagner et al., 1999b; Naeimi et al., 2009). In this study, the ASCAT soil moisture products of the WARP version 5.5 (release 1.2) of the retrieval algorithm were used (https://rs.geo.tuwien.ac.at/products).

Wagner et al. (1999b) proposed a method to calculate the SSM content from the backscattering measurements at a reference angle of 40°, using the lowest (dry) and highest (wet) values over a long period. The SSM content m_s is estimated by a processing step, using

$$m_s = \frac{\sigma^0 - \sigma^0_{dry}}{\sigma^0_{wet} - \sigma^0_{dry}} \tag{2}$$

where σ^0_{dry} and σ^0_{wet} represent the backscattering values at completely dry and wet conditions, and σ^0 is the present backscatter measurement. Soil moisture variations are adjusted between the historically lowest (0%) and highest (100%) values, producing a time series of relative soil moisture for the topmost centimeters of the soil (Wagner et al., 1999b, 2007). In order to estimate the root-zone profile soil moisture, the semi-empirical approach proposed by Wagner et al. (1999b), also called an exponential filter, is used to obtain the SWI values from the SSM, m_s.

$$SWI(t) = \frac{\sum_i m_s(t_i) \cdot e^{-\frac{t-t_i}{T}}}{\sum_i e^{-\frac{t-t_i}{T}}} \quad \text{for} \quad t_i < t \qquad (3)$$

The SWI at time t, $m_s(t_i)$ is the SSM estimated from remote sensing at time t_i. T is the characteristic time length, in units of day. In this study, we used SWI values at T = 1, 5, 10, 15, and 20 to compare with the root zone soil moisture contents (in situ data at 20, 30, and 50cm and USDA AMSR-E) in Table 8. In particular, we compared the in situ data (20 cm) and SWI values at T=5 based on maximizing the correlation with in-situ root zone soil moisture measurements during the growing seasons (May 1 through September 30, 2010).

3. Methods

The passive (AMSR-E) and the active (ASCAT) sensor soil moisture products, the C- and X-band observations, represent a layer depth of 2cm (Naeimi & Wagner, 2010, Escorihuela et al., 2010), were compared with *in situ* observations at depths of 10, 20, 30, and 50 cm. ASCAT and AMSR-E soil moisture products are characterized by different measurement units. AMSR-E products are expressed as volumetric values (m^3m^{-3} or g/cm^3), in absolute terms. On the other hand, ASCAT products are relative concept, represented by a degree of saturation between 0 and 100%. We suggested a simplistic equation to rescale the ASCAT product, based on the physical concept, the effective saturation (s_e), of the Green-Ampt infiltration model (Brooks & Corey, 1964; Rawls et al., 1983). To solve for the systematic differences between the remotely sensed SM and the *in situ* measurements, the linear regression correction (REG), mean/standard-deviation ($\mu - \sigma$) matching, and cumulative distribution function (CDF) matching approaches are implemented (Albergel et al., 2012; Brocca et al., 2011; Draper et al., 2009; Jackson et al., 2010; Lacava et al., 2010; Liu et al., 2011; Su et al., 2013; Scipal et al., 2008).

3.1 Effective saturation of soil texture classes

The concept of effective saturation (s_e) (Brooks & Corey, 1964; Rawls et al., 1983) was employed in order to compare ASCAT soil moisture values (degree of saturation, %) with AMSR-E soil moisture contents (volumetric units, m^3/m^3). The ASCAT soil moisture data are relative values, which are estimated according to the degree of the difference between the saturated and residual water contents. In this study, the ASCAT SSM content was rescaled from the degree of saturation (%) to the volumetric units (m^3/m^3) by considering the soil porosity (Wagner et al., 2013). The ASCAT SWI was estimated by factoring in the residual water content (θ_r) as well, rather than just the total porosity (η). This is because SWI is one of the RZSM index which should consider the residual water content as a characteristic of the root zone soil.

$$s_e = \frac{\theta - \theta_r}{\eta - \theta_r} = \frac{\theta - \theta_r}{\theta_e} \quad (4)$$

where s_e = effective saturation, θ = soil moisture content, θ_r = residual water content, and η = total porosity. The effective saturation (s_e) is the ratio of the available moisture, $\theta - \theta_r$, to the maximum possible available moisture content, $\eta - \theta_r$, where $\eta - \theta_r$ is called the effective porosity θ_e. The effective saturation (s_e) has a range of $0 \leq s_e \leq 1.0$, provided $\theta_r \leq \theta \leq \eta$. If the specific area is saturated by rainfall, the *in situ* soil moisture content will become equal to the total porosity (η) at that time; while during completely dry time, the soil moisture becomes the residual water content (θ_r). Rawls et al. (1983) showed that the effective porosity (θ_e) depends on the soil texture class. We assumed that the ASCAT's historically lowest and highest values were the residual water content (θ_r) and effective saturation (s_e), respectively. The rescaled ASCAT values $\theta_{ASCAT_{rescaled}}$ were calculated by:

$$\theta_{ASCAT_{rescaled}} = (\theta_{ASCAT_{original}} \cdot \theta_e + \theta_r) / 100 \quad (5)$$

where $\theta_{ASCAT_{original}}$ is the original ASCAT soil moisture data (degree of saturation, %), and $\theta_{ASCAT_{rescaled}}$ is the rescaled ASCAT soil moisture data (volumetric soil moisture contents, m^3/m^3). The rescaled values were able to compare between ASCAT and other passive sensor products or *in situ* measurements, expressed as volumetric soil moisture contents (m^3/m^3). The ASCAT data was rescaled from the percentage of saturation to the volumetric unit by considering the effective saturation and residual water contents. We selected a dominant soil texture within the each footprint from the Korean soil information system (http://soil.rda.go.kr). The rescaled ASCAT datasets applied by this method can be more accurately converted than the datasets using just total porosity, though there are somewhat uncertainties due to the wide range of the effective porosity and residual water contents, even amongst the same soil type. Therefore, we applied the concept of effective saturation to the

ASCAT SWI data, prior to the renormalization methods using the Green and Ampt infiltration parameters, with typical ranges of η , θ_r and θ_e according to the soil texture classes (Rawls et al., 1983).

3.2 Comparison metrics

A two-dimensional Taylor diagram (Taylor, 2001) is used to represent multiple statistics for an inter-comparison between satellite soil moisture products and *in situ* data on a plot. The SDV and E are given by:

$$SDV = \frac{stdev_{SM_{satellite}}}{stdev_{SM_{in-situ}}} \tag{6}$$

$$E^2 = \frac{RMSE^2 - Bias^2}{stdev^2_{SM_{in-situ}}} \tag{7}$$

$$E^2 = SDV^2 + 1 - 2 \cdot SDV \cdot R \tag{8}$$

SDV is the normalized standard deviation that indicates the ratio between the satellite data and *in situ* measurements. In this diagram, the *SDV* and *R* values are shown as a radial distance and an angle respectively, and the *in situ* observation is displayed as a point on the x axis at *R* = 1 and *SDV*=1. The centered root mean square error (*E*) between the satellite and *in situ* soil moisture, which is normalized by $stdev_{SM_{in-situ}}$, the standard deviation of the *in situ* observations, is the distance to this point. This diagram has been in previous researches for comparison and for validation studies related to satellite-based products (de Rosnay et al., 2009; Albergel et al., 2012; Liu & Xie, 2013).

The three following statistical indexes are used to estimate the satellite soil moisture product accuracy:

$$Bias = \overline{\sum SM_{satellite} - SM_{in-situ}} \quad (9)$$

$$RMSE = \sqrt{\overline{\sum (SM_{satellite} - SM_{in-situ})^2}} \quad (10)$$

$$R = \sqrt{1 - \frac{\sum (SM_{satellite} - SM_{in-situ})^2}{\sum (SM_{in-situ} - \overline{SM_{in-situ}})^2}} \quad (11)$$

where *Bias* is the mean value of the differences for each time, and *RMSE* is the root mean squared error between the *in situ* soil moisture measurements, $SM_{in-situ}$, and the satellite soil moisture product, $SM_{satellite}$. *R* is the correlation coefficient.

3.3 Renormalization methods: Linear regression correction, $\mu-\sigma$ and CDF matching

Three renormalization strategies are implemented in order to make inter-comparisons between different satellite soil moisture products. The first approach, linear regression correction (Jackson et al., 2010; Brocca et al., 2011), is based on a linear regression equation between the satellite and *in situ* soil moisture values. Standard linear regression minimizes the squared-differences between satellite-data and in situ data (i.e., providing the least-square solution that minimizes the residual). It provides the match of the satellite data to the in situ data in the least-square sense, under the assumption that measurement errors are absent in the in situ data (Su et al., 2014). The second average - standard deviation ($\mu - \sigma$) matching (Draper et al., 2009, Su et al., 2013), matches their means and variances using:

$$\hat{\vartheta}_s = \mu_i + \frac{\sigma_i}{\sigma_s}(\vartheta_s - \mu_s) \quad (12)$$

where $\hat{\vartheta}_s$ = Normalized satellite data, μ_i = mean values of the *in situ* data, σ_i = standard deviations of the *in situ* data, σ_s = standard deviations of the satellite data, ϑ_s = satellite data, and μ_s = mean values of the satellite data. Lastly, the CDF matching (Reichle & Koster, 2004; Drusch et al., 2005; Scipal et al., 2008; Lacava et al., 2010; Liu et al., 2011; Brocca et al., 2011; Albergel et al., 2012; Su et al., 2013) is a non-linear method used to remove systematic differences between two datasets, and to match the CDF of the satellite retrievals to the CDF of the *in situ* soil moisture. The CDF matching approach was applied to each grid individually, enabling us to efficiently remove the bias and variance error in the local grid. Liu et al. (2011) applied a piece-wise linear CDF matching, dividing the CDF curve into 12 segments. In this study, CDF method is applied to the ASCAT and AMSR-E (NSIDC, VUA-NASA, USDA) products using the EasyFIT application. This method was used as a data analysis tool, allowing us to match one satellite data to *in-situ* data by using the corresponding cumulative distributions, respectively. The user can select the best CDF model depending on the chosen goodness of fit tests and use this CDF model to renormalize the investigated satellite data (http://www.mathwave.com/help/easyfit/index.html).

It should be noted that these renormalization approaches have the possibility of generating artificial biases and thus become regarded a sub-optimal works in order to remove the biases (Yimaz and Crow, 2013; Su et al., 2014). If certain conditions for datasets were met (mutual linear relationship, independence of errors, and long enough datasets), it would be optimal to use the triple collocation analysis (TCA) based rescaling factors and the lagged variables (LV) method in hydrological assimilation studies (Yilmaz and Crow, 2013; Su et al., 2014). In this study, despite the fact that the three rescaling methods (REG, $\mu - \sigma$, and CDF) provide only approximations as the sub-optimal estimation, they can be used to assess the accuracy of satellite soil moisture retrievals and inter-compare between different satellite products, proven by as previous studies (Brocca et al., 2011; Su et al., 2013).

4. Results and discussion

4.1 Evaluation of AMSR-E surface soil moisture (NSIDC, VUA-NASA)

The two AMSR-E soil moisture products developed by the NSIDC and VUA-NASA were validated using the *in situ* measurements (10 cm) provided by the KMA and HSC for the study period of 2010 (May 1 to September 30), at nine sites located on the Korean peninsula. The pixel values representing each ground measurement site were extracted from satellite based soil moisture products. Temporal variations of the SSM for the NSIDC, VUA-NASA and ASCAT products and the RZSM for the NSIDC SWI, USDA and ASCAT SWI products *in situ* data are given in Figs. 2a and b.

Fig. 2a shows that the NSIDC AMSR-E SSM products only reacted slightly to the rainfall events, compared with the other soil moisture products and were underestimated. The NSIDC soil moisture showed mean values ranging from 0.09 to 0.14 m^3/m^3, and standard deviations of the soil moisture ranging from 0.01 to 0.02 m^3/m^3. This low temporal variability and underestimated patterns of the NSIDC soil moisture had been previously found by several NSIDC AMSR-E validation studies (Wagner et al., 2007; Gruhier et al., 2008; Jackson et al., 2010; Choi, 2012). In particular, these results corresponded with those of Choi (2012), which validated the AMSR-E product using ground based measurements and the Common Land Model (CLM), for two major land cover types in Korea. The correlation coefficients between the NSIDC products and *in situ* measurement values ranged from 0.11 to 0.61 (Average = 0.39). Table 3 shows that biases ranged from -0.14 to 0.02 (Average = -0.05 m^3/m^3), while the RMSE ranged from 0.02 to 0.16 (Average = 0.08 m^3/m^3).

We evaluated the accuracy of the VUA-NASA soil moisture products (C- and X-band), by comparing them with ground based measurements, according to ascending / descending pass. It is worthy of note that the C-band VUA-NASA data have higher correlation than the X-band data for all of the sites (Table 4). This implies that the C-band soil moisture products were more reliable than the X-band products, which are further recommended for use in northeast Asia, where RFI was observed (Njoku et al., 2005). It is also worth noting that the ascending AMSR-E data had good agreement with the ground-based measurements compared with the descending data, regardless of the band type in this study (Table 4). These results supported the findings of Loew et al. (2009) and Brocca et al. (2011). Brocca et al. (2011) pointed out that ascending AMSR-E data provided higher correlations with site-specific data in Europe because the ascending passes (day-time) data had the vegetation transparent effects by high temperatures during the day.

Considering the results of Fig. 2a, the VUA-NASA soil moisture products (C-band and descending pass) clearly responded to rainfall events and showed reasonable agreement with the ground-based measurements in contrast to the NSIDC soil moisture products. In these graphs, we can see the temporal variations, as the values increased during rainfall and decreased after rainfall events. While the *in situ* soil moisture ranged from 0.11 to 0.27 m^3/m^3, the VUA-NASA soil moisture showed higher average values, ranging from 0.33 to 0.44 m^3/m^3 (Table 3). The standard deviations of the *in situ* soil moisture measurements ranged from 0.03 to 0.05 m^3/m^3. The VUA-NASA products had a higher standard deviation, ranging from 0.07 to 0.13 m^3/m^3. The correlation coefficients ranged from 0.19 to 0.60 (Average: 0.42), the biases ranged from 0.10 to 0.27 (0.20 m^3/m^3), and the RMSE ranged from 0.13 to 0.29 (Average: 0.22 m^3/m^3).

These results match up with several recent studies that VUA-NASA products were better correlated with ground soil moisture measurements than NSIDC products, and implied that AMSR-E data was suited to VUA-NASA soil moisture retrieval, and that long wavelengths (C-band) penetrated deeper into vegetation and soil than short wavelengths (X-band) (Choi, 2012; Draper et al., 2009; Rudiger et al., 2009; Wagner et al., 2007). In comparison with previous studies, the correlation between the VUA-NASA soil moisture and *in situ* measurements in this study area was lower than for other regions, such as America (Jackson et al., 2010), Europe (Wagner et al., 2007), West Africa (Gruhier et al., 2010) and Australia (Draper et al., 2009; Su et al., 2013). These results suggest that northeast Asia including the Korean peninsula is more affected by RFI as well as relatively heterogeneous land cover within the footprint than these validated sites (Choi, 2012).

4.2 Evaluation of AMSR-E root zone soil moisture (NSIDC SWI, USDA)

The NSIDC AMSR-E RZSM products were calculated using the exponential filter method in order to compare other RZSM products (USDA and ASCAT SWI). The NSIDC SWI showed that the average and standard deviation values ranged from 0.09 to 0.14 m^3/m^3, and 0.00 to 0.02 m^3/m^3, respectively (Table 5). The correlation coefficients between these products and the *in situ* measurement values (20 cm) ranged from 0.16 to 0.72 (Average: 0.47). The NSIDC SWI products had higher correlation values than the NSIDC SSM products (0.39) for all of the sites, with the exception of Suwon. These results are slightly better than a previous study that was performed in Europe (Brocca et al., 2011), which showed that the average R values of the NSIDC SWI products were equal to 0.45 and 0.20 with *in situ* measurements at 5 cm (surface) and 10-30 cm (root zone), although modified by the application of CDF matching method, respectively.

The AMSR-E RZSM is derived by the USDA, via the assimilation of VUA-NASA soil moisture retrievals into the 2-Layer Palmer Water Balance Model, using the Ensemble Kalman filter (EnKF). We executed a correlation analysis between the *in situ* soil moisture (10, 20, 30, and 50 cm) and USDA RZSM, in order to confirm which depth has the highest correlation coefficients. As this dataset was designed to only use the C-band soil moisture at a descending overpass time (1:30 am), *in situ* measurements were also extracted at the same time. Fig. 2b shows that the USDA products overestimate the soil moisture, and have a large bias, as compared to the *in situ* measurements. The biases ranged from 0.14 to 0.40 m^3/m^3 (Average: 0.28 m^3/m^3), and the RMSE ranged from 0.15 to 0.41 (Average: 0.29) in Table 5. The USDA soil moisture showed that the average and standard deviations values ranged from 0.40 to 0.61 m^3/m^3, and 0.04 to 0.10 m^3/m^3, respectively. Table 8 shows the correlation coefficient values between the USDA RZSM and the *in situ* soil moisture measurements at nine sites. The average R values were equal to 0.70, 0.72, 0.64 and 0.52, at 10, 20, 30, and 50 cm depth, respectively. In particular, the R values at 20 cm depth ranged from 0.47 to 0.88 (Average: 0.72), showing the highest R-values of all of the AMSR-E products. Most of the study sites had good correlation coefficients at depths of 10 and 20 cm. The highest R values (r = 0.83 and 0.88) were obtained at 10 and 20 cm depths in the Cheongju site. Conversely, the lowest R values (r = 0.37 and 0.45) were obtained at 30 and 50 cm depths in Seosan site. This implied that there were differences in correlation coefficient values of the USDA RZSM products according to the depths of the *in situ* measurements and land surface characteristics. Furthermore, it can be inferred that the USDA RZSM products best correlate with the *in-situ* measurements at about 20 cm depths.

4.3 Evaluation of ASCAT surface and root zone soil moisture products

The ASCAT surface soil moisture (SSM) was validated for nine sites in Korea. Fig. 2a shows the time series of ASCAT SSM products versus the two AMSR-E and ground based data at a

10 cm depth for all of the sites. Notwithstanding the high temporal variability of the SSM, the ASCAT products corresponded more accurately with the temporal patterns of the *in situ* measurements than did the AMSR-E SSM products during the growing season. The ASCAT products showed that the average and standard deviations values ranged from 0.14 to 0.34 m^3/m^3, and 0.05 to 0.08 m^3/m^3, respectively (Table 6). Correlation coefficients between these products and the *in situ* measurement values (10 cm) ranged from 0.41 to 0.70 (Average: 0.53). The ASCAT SSM products had higher average correlation values than did the two AMSR-E SSM products (NSIDC: 0.39, VUA-NASA: 0.42). These results correspond with previous studies (Brocca et al., 2011; Liu et al., 2011). The ASCAT soil water index (SWI) is one of the RZSM values (Naeimi and Wagner, 2010; Brocca et al., 2011). We applied the concept of effective saturation to the ASCAT SWI products according to soil texture. The time series in Fig. 2b show that the temporal patterns of the rescaled ASCAT SWI are more similar to those of the *in situ* measurements, than the AMSR-E products. Fig. 4 shows a comparison between the ground measurements at 20cm depth and the ASCAT SWI products with the average, standard deviation, bias and RMSE. The rescaled ASCAT SWI values corresponded with the ground measurement as the average values of the *in situ* soil moisture measurements for the nine sites were 0.21 m^3/m^3 during the growing season and the average value for the ASCAT SWI is 0.27 m^3/m^3. The average correlation coefficient value was equal to 0.75. The biases ranged from -0.08 to 0.21 (0.06 m^3/m^3), and the RMSE ranged from 0.04 to 0.21 (0.11 m^3/m^3), as shown in Table 7. These results indicate that the rescaled ASCAT product is more accurate than the AMSR-E products, nearly to the target value of 0.04 m^3/m^3, which was the numerical goal of the SMAP mission (Entekhabi et al., 2010b). It is worthy to note that the ASCAT SWI values should be evaluated so as to determine an effective saturation concept with a renormalization method, as has been used in several previous studies (Brocca et al., 2011; Draper et al., 2009; Su et al., 2013).

We also analyzed the correlation values between the *in situ* soil moisture measurements (10, 20, 30, and 50 cm) and the ASCAT SWI data, according to the characteristic time length, T (Table 8). Generally, the ASCAT SWI has relatively good correlation coefficients with the *in situ* RZSM at 10 and 20 cm, compared with 30 and 50 cm. The highest average R-value (0.75) at T = 5 days was obtained for the depths of 10 and 20 cm. This may be due to the length of time (T), which connotes the infiltration time. There are horizontal variations in the amount of soil moisture contents after rainfall events, which are caused by the differences in infiltration velocity, according to the type of soil texture. The differences in R-values among the nine study sites were found in Table 8. In particular, the Suwon and Seosan sites had the lowest R-values at T = 10, 15 and 20 days for the depth of 10 cm. This may be partly explained by the spatial heterogeneity of land cover within the foot-print compared to other sites (Fig. 1). Dominant land cover types in pixel may be the cause of the problematic retrieval results (Lakhankar et al., 2009; Loew, 2008; van de Griend et al., 2003). Loew (2008) mentioned that the quality of the soil moisture retrievals was influenced by the spatial heterogeneity within a resolution pixel, especially concerning vegetation, urban, and open water surfaces, and might ultimately result in significantly biased soil moisture retrievals.

4.4 Inter-comparison of satellite soil moisture retrievals

Fig. 2 shows the temporal profiles of the satellite based soil moisture products (SSM: NSIDC, VUA-NASA, and ASCAT, RZSM: NSIDC SWI, USDA, and ASCAT SWI) for the nine different locations. All of the products responded to the multiple rainfall events during the growing season in 2010. However, there were significant differences between the three satellite-based SSM datasets. The R-values of the satellite-based SSM datasets are in the range of 0.11-0.61, 0.19-0.60 and 0.41-0.70, with average values of 0.39, 0.42, and 0.53, for the NSIDC, VUA-NASA AMSR-E and ASCAT datasets, respectively (Fig. 3a). The ASCAT had the highest mean correlation (R=0.53), compared to the other satellite datasets. Fig. 3b shows the comparison of the RMSE between the satellite soil moisture products (AMSR-E and ASCAT). The RMSE of the modified datasets are in the range of 0.02-0.16, 0.13-0.29, and 0.06-0.22 m^3/m^3, with average values of 0.08, 0.22, and 0.10 m^3/m^3, for the NSIDC, VUA-NASA AMSR-E and ASCAT datasets, respectively. NSIDC AMSR-E had lowest RMSE values, followed by the ASCAT, and VUA-NASA AMSR-E, in spite of the locational differences. The ASCAT products were applied with the concept of soil porosity (Wagner et al., 2013). These results are different than the results of several previous studies, in that the RMSE between the VUA-NASA and *in situ* data was smaller than the RMSE between the NSIDC and *in situ* data (Wagner et al., 2007; Choi, 2012). However, these findings are similar to those of Gruhier et al. (2010), as they showed that the RMSE of the NSIDC data (0.05 m^3/m^3) was smaller than that of the VUA-NASA data (0.06 m^3/m^3) during monsoon seasons; however, the RMSE of the NSIDC data (0.07 m^3/m^3) was bigger than that of the VUA-NASA data (0.02 m^3/m^3) during dry seasons.

Fig. 4a shows that R-values of satellite based RZSM datasets. These average values were 0.47, 0.72, and 0.75, for the NSIDC SWI, USDA AMSR-E and ASCAT SWI datasets, respectively. The RMSE of these datasets ranged from 0.02-0.20, 0.15-0.41, and 0.04-0.21 m^3/m^3, with the average values of 0.10, 0.29, and 0.11 m^3/m^3 (Fig. 4b). The ASCAT also has the highest mean correlation (R=0.75), compared to the other satellite datasets. The results of the comparisons for the following sets were modified by the application of renormalization approaches, REG, $\mu-\sigma$, and CDF matching, and were subsequently categorized according to satellite products (SSM and RZSM) 1) NSIDC, VUA-NASA AMSR-E, and ASCAT SSM, and 2) NSIDC SWI, USDA AMSR-E, and ASCAT SWI products. There are several causes of various systematic differences (Bias, RMSE). These errors may be caused due to the fact that the microwave sensor on board the satellite can detect only the soil moisture in the top soil layer (2-5 cm), and satellite-derived soil moisture contents are easily affected by various atmospheric forcing. Furthermore, the satellite data represents the spatial average value, while the *in situ* measurement data reflect sites that were monitored at certain depths (Draper et al., 2009).

Fig. 5 shows four Taylor diagrams that illustrate the statistics for the comparison between NSIDC, VUA-NASA, and ASCAT SSM data and ground based measurement data (10 cm) for the original and three renormalization methods, REG, $\mu - \sigma$, and CDF matching. On average, for the nine sites, the R-values of the three renormalized satellite soil moisture products were 0.39, 0.42 and 0.53 (REG and $\mu - \sigma$) and 0.38, 0.43, and 0.55 (CDF), for NSIDC, VUA-NASA AMSR-E, and ASCAT datasets, respectively. All of the symbols representing the NSIDC data (red dots) are located just below the SDV value of 1 (violet dotted line in Fig. 5a). This implies that the temporal variability of the NSIDC data is lower, than that of the other satellite products. Fig. 5b shows the Taylor diagram representing REG-based rescaling. As seen in this figure, the average SDV values modified from 0.32, 2.43, and 1.56 to 0.36, 0.42, and 0.53 m^3/m^3 for all of the products. The REG method showed SDV values less than one for all of the products, drawing a semicircle. The ASCAT data (Green dots) presents relatively close to the x axis at R = 1 and SDV=1, followed by VUA-NASA, and NSIDC. These obtained SDV values were equal to R-values. The results using the Average – Standard deviation ($\mu - \sigma$) matching method showed that all of the SDV values were equal to 1 (Fig. 5c). Therefore, this method enables us to compare three satellite products only considering correlation coefficients. Fig. 5d shows the dispersion of statistics, which were modified using the CDF matching method. This diagram depicts the fact that most of the data points are close to the SDV value of 1, except for some of the NSIDC products.

The four Taylor diagrams of the RZSM products, which illustrate the statistics of the comparison between NSIDC SWI, USDA, and ASCAT SWI data and ground-based measurement data (20 cm) for the original and three renormalization methods (REG, $\mu - \sigma$, and CDF matching) are shown in Fig. 6. In general, the RZSM correlations had better results than the SSM correlations. The R-values of the three satellite soil moisture products were 0.47, 0.72 and 0.75 for the NSIDC SWI, USDA, and ASCAT SWI datasets, respectively. Throughout the three renormalization methods, the RMSE values improved from 0.10, 0.29, and 0.11 to 0.03, 0.02, and 0.02 m^3/m^3 (REG), 0.03, 0.03, and 0.02 m^3/m^3 ($\mu - \sigma$), and 0.04, 0.03, and 0.02 m^3/m^3 (CDF), respectively. As seen in Fig. 6c, the $\mu - \sigma$ method showed that all satellite RZSM products followed the curve, SDV = 1 (violet dotted line). The CDF matching method was able to acquire the SDV values of three RZSM products close to 1 (Fig. 6d). Through four diagrams, we can assess that the ASCAT SWI and USDA RZSM products outperform the NSIDC SWI products. Furthermore, the ASCAT SWI data are more accurate than USDA RZSM data in Fig. 6d. Basically, the result may be due to the fine resolution of the 0.125° grid of the ASCAT products, compared to the AMSR-E products, which have a 0.25° grid, and the application of the exponential filter which allows satellite products to be comparable with *in situ* observations of near-surface soil moisture. Subsequent research is required not only to assess the applicability of ASCAT with Advanced Microwave Scanning Radiometer 2 (AMSR2) for the different regions in east Asia, but also to validate and calibrate upcoming SMAP products.

5. Summary and conclusions

Several soil moisture datasets from active / passive microwave sensors have been provided to users for diverse public purposes. The validation and evaluation of these products are required on both a global and local scale. In this study, active (ASCAT) and passive (AMSR-E) sensor products were estimated from nine stations located in the Korea peninsula, in northeast Asia. Through this validation study, we were able to conclude that ASCAT, a type of active microwave sensor, outperformed the three AMSR-E products (NSIDC, VUA-NASA and USDA) in terms of both SSM and RZSM products in northeast Asia. We rescaled ASCAT products considering the concept of effective saturation. In addition, the AMSR-E USDA RZSM showed characteristics related to soil texture. Through the comparison of soil moisture retrievals with three renormalization methods (REG, $\mu - \sigma$ and CDF matching) using a Taylor diagram, the ASCAT satellite datasets proved their reliability in terms of both SSM and RZSM. This study would play an important role in assessing global satellite-based soil moisture under the circumstances, where other major satellite soil moisture products have limitations such as the Soil Moisture Ocean Salinity (SMOS) due to the RFI in northeast Asia, and the AMSR-E instrument onboard the Aqua satellite, which stopped producing data after October 2011, due to an antenna problem. Furthermore, such research might lead to a better understanding of operational hydrological investigations and water management activities, as well as in validating and estimating remotely sensed soil moisture products derived by Metop-B, AMSR2, and the upcoming SMAP mission.

Acknowledgements

We thank two anonymous reviewers and Jongjin Baek for their constructive comments on the manuscript. This research was supported by the Basic Science Research Program, through the National Research Foundation of Korea (NRF), funded by the Ministry of Education, Science and Technology (2013-0004743). AMSR-E soil moisture data were obtained from the “NASA Global Change Master Directory Date Sets”, and “National Snow & Ice Data

Center". ASCAT soil moisture data were produced by the Vienna University of Technology (TU-WIEN). We would also like to thank the Korea Meteorological Administration (KMA) and Hydrological Survey Center (HSC) for providing ground soil moisture data.

References

Albergel, C., de Rosnay, P., Gruhier, C., Muñoz-Sabater, J., Hasenauer, S., Isaksen, L., et al. (2012). Evaluation of remotely sensed and modelled soil moisture products using global ground-based in situ observations. *Remote Sensing of Environment*, 118, 215–226.

Albergel, C., Rüdiger, C., Pellarin, T., Calvet, J. -C., Fritz, N., Froissard, F., et al. (2008). From near-surface to root-zone soil moisture using an exponential filter: An assessment of the method based on in situ observations and model simulations. *Hydrology and Earth System Sciences*, 12, 1323–1337, doi:10.5194/hess-12-1323-2008.

Bartalis, Z., Wagner, W., Naeimi, V., Hasenauer, S., Scipal, K., Bonekamp, H., et al. (2007). Initial soil moisture retrievals from the METOP-A Advanced Scatterometer (ASCAT). *Geophysical Research Letters*, 34, L20401. http://dx.doi.org/10.1029/2007GL031088.

Bindlish, R., Crow, W. T., & Jackson, T. J. (2009). Role of passive microwave remote sensing in improving flood forecasts. *IEEE Geoscience and Remote Sensing Letters*, 6(1), 112–116.

Bolten, J. D., & Crow, W. T. (2012). Improved prediction of quasi-global vegetation conditions using remotely-sensed surface soil moisture, *Geophysical Research Letter*, 39, L19406, doi:10.1029/2012GL053470.

Bolten, J. D., Crow, W. T., Zhan, X., Jackson, T. J., & Reynolds, C. A. (2010). Evaluating the utility of remotely sensed soil moisture retrievals for operational agricultural drought monitoring. *IEEE Journal of Selected Topics in Applied Earth Observations and Remote Sensing*, 3(1), 57–66. http://dx.doi.org/10.1109/JSTARS.2009.2037163.

Brocca, L., Hasenauer, S., Lacava, T., Melone, F., Moramarco, T., Wagner, W., Dorigo, W., Matgen, P., Martínez-Fernández, J., Llorens, P., Latron, J., Martin, C., & Bittelli, M. (2011). Soil moisture estimation through ASCAT and AMSR-E sensors: An intercomparison and validation study across Europe. *Remote Sensing of Environment*, 115(12), 3390–3408.

Brocca, L., Melone, F., Moramarco,T., Wagner,W., & Hasenauer, S. (2010). ASCAT Soil Wetness Index validation through in-situ andmodeled soilmoisture data in central Italy. *Remote Sensing of Environment*, 114(11), 2745–2755, doi:10.1016/j.rse.2010.06.009.

Brocca, L., Melone, F., Moramarco, T., Wagner, W., Naeimi, V., Bartalis, Z., et al. (2010). Improving runoff prediction through the assimilation of the ASCAT soil moisture product. *Hydrology and Earth System Sciences*, 14(10), 1881–1893.

Brocca, L., Morbidelli, R., Melone, F., & Moramarco, T. (2007). Soil moisture spatial variability in experimental areas of central Italy. *Journal of Hydrology*, 333(2–4), 356−373.

Brocca, L., Moramarco, T., Melone, F., Wagner, W., Hasenauer, S., & Hahn, S. (2012). Assimilation of surface and root-zone ASCAT soil moisture products into rainfall-runoff modelling. *IEEE Transactions on Geoscience and Remote Sensing*, 99, 1–14.

Brooks, R. H., & Corey, A. T. (1964). Hydraulic properties of porous media, *Hydrology papers. 3*, Colorado State University.

Cho, E., & Choi, M. (2014). Regional scale spatio-temporal variability of soil moisture and its relationship with meteorological factors over the Korean peninsula. *Journal of Hydrology*. http://dx.doi.org/10.1016/j.jhydrol.2013.12.053.

Choi, M. (2012). Evaluation of multiple surface soil moisture for Korean regional flux monitoring network sites: Advanced Microwave Scanning Radiometer E, land surface model, and ground measurements. *Hydrological Processes*, 26(4), 597–603.

Choi, M., & Hur., Y. (2012). A microwave-optical/infrared disaggregation for improving spatial representation of soil moisture using AMSR-E and MODIS products. *Remote Sensing of Environment*, 124, 259-269.

Choi, M., & Jacobs, J. M. (2007). Soil moisture variability of root zone profiles within SMEX02 remote sensing footprints. *Advances in Water Resources*, 30(4), 883–896.

de Jeu, R.A.M., T.R.H. Holmes, R.M. Parinussa, M. Owe (2014). A spatially coherent global soil moisture product with improved temporal resolution, *Journal of Hydrology*, in press, doi:10.1016/j.jhydrol.2014.02.015.

de Rosnay, P., Drusch, M., Boone, A., Balsamo, G., Decharme, B., Harris, P., et al. (2009). AMMA land surface model intercomparison experiment coupled to the community microwave emission model: ALMIP-MEM. *Journal of Geophysical Research*, 114, D05108.

Dobson, M. C. & Ulaby, F. T. (1986). Active microwave soil moisture research. *IEEE Transaction on Geoscience and Remote Sensing*, GE-24, 23-35.

Draper, C. S., Walker, J. P., Steinle, P. J., de Jeu, R. A.M., & Holmes, T. R. H. (2009). An evaluation of AMSR-E derived soil moisture over Australia. *Remote Sensing of Environment*, 113, 703–710. http://dx.doi.org/10.1016/j.rse.2008.11.011.

Drusch, M., Wood, E. F., & Gao, H. (2005). Observation operators for the direct assimilation of TRMM microwave imager retrieves soil moisture. *Geophysical Research Letters*, 32, L15403, doi:10.1029/2005GL023623.

Entekhabi, D., Njoku, E. G., O'Neill, P. E., Kellogg, K. H., Crow, W. T., Edelstein, W. N., et al. (2010a). The SoilMoisture Active and Passive (SMAP) mission. *Proceedings of the IEEE*, 98(5), 704–716.

Entekhabi, D., Reichle, R. H., Koster, R. D., & Crow, W. T. (2010b). Performance metrics for soil moisture retrievals and application requirements. *Journal of Hydrometeorolgy,* 11, 832–840, doi:10.1175/2010JHM1223.1.

Escorihuela, M. J., Chanzy, A., Wigneron, J. P., & Kerr, Y. H. (2010). Effective soil moisture sampling depth of L-band radiometry: A case study. *Remote Sensing of Environment*,114, 995–1001, doi:10.1016/j.rse.2009.12.011.

Famiglietti, J. S., Ryu, D., Berg, A. A., Rodel, M., & Jackson, T. J. (2008). Field observations of soil moisture variability across scales. *Water Resources Research*, 44, W01423.

Gruhier, C., de Rosnay, P., Hasenauer, S., Holmes, T., de Jeu, R., Kerr, Y., Mougin, E., Njoku, E., Timouk, F., Wagner, W., & Zribi, M. (2010). Soil moisture active and passive microwave products: intercomparison and evaluation over a Sahelian site, *Hydrology and Earth System Sciences*, 14, 141–156, doi:10.5194/hess-14-141-2010.

Gruhier, C., de Rosnay, P., Kerr, Y., Mougin, E., Ceschia, E., Calvet, J-C. (2008). Evaluation of AMSR-E soil moisture product based on ground measurements over temperate and semi-arid regions. *Geophysical Research Letters*, 35, L10405. doi: 10.1029/2008GL033330.

Jackson, T. J., Cosh, M. H., Bindlish, R., Starks, P. J., Bosch, D. D., Seyfried, M., Goodrich, D. C., Moran, M. S., & Du, J. (2010). Validation of advanced microwave scanning radiometer soil moisture products. *IEEE Transactions on Geoscience and Remote Sensing*, 48(12), 4256–4272.

Jackson, T. J., Hsu, A. Y., & O'Neill, P. E. (2002). Surface soil moisture retrieval and mapping using high-frequency microwave satellite observations in the Southern Great Plains. *Journal of Hydrometeorology*, 3, 688–699.

Jackson, T. J., Schmugge, T. J., & Engman, E. T. (1996). Remote sensing applications to hydrology: soil moisture, *Hydrological Sciences Journal*, 41(4), 517-530.

Jacobs, J. M., Mohanty, B. P., Hsu, E. -C., & Miller, D. (2004). SMEX02: Field scale variability, time stability and similarity of soil moisture. *Remote Sensing of Environment*, 92, 436−446.

Kerr, Y. H., Waldteufel, P., Richaume, P., Wigneron, J. P., Ferrazzoli, P., Mahmoodi, A., et al. (2012). The SMOS soil moisture retrieval algorithm. *IEEE Transactions on Geoscience and Remote Sensing*, 50(5), 1384–1403.

Kim, B.-J., Kripalani, R.H., Oh, J.-H., Moon, S.-E. (2002). Summer monsoon rainfall patterns over South Korea and associated circulation features. *Theoretical and Applied Climatology*, 72 (1–2), 65–74. doi: 10.1007/s007040200013

KMO (2006). Annual Climatological Report, *Korea Meteorological Administration*, 11–1360000-000016-10.

Lacava, T., Brocca, L., Calice, G., Melone, F., Moramarco, T., Pergola, N., & Tramutoli, V. (2010). Soil moisture variations monitoring by AMSU-based soil wetness indices: A long-term inter-comparison with ground measurements. *Remote Sensing of Environment*, 114(10), 2317–2325, doi:10.1016/j.rse.2010.05.008.

Lakhankar, T., Ghedira, H., Temimi, M., Azar, A.E., Khanbilvardi, R. (2009). Effect of land cover heterogeneity on soil moisture retrieval using active microwave remote sensing data. *Remote Sensing*, 1, 80–91.

Leroux, D. J., Kerr, Y. H., Richaume, P., Fieuzal, R. (2013). Spatial distribution and possible sources of SMOS errors at the global scale, *Remote Sensing of Environment*, 133, 240-250

Liu, Y. Y., Dorigo, W. A., Parinussa, R.M., de Jeu, R. A. M., Wagner, W., McCabe, M. F., Evans, J. P., & van Dijk, A. I. J. M. (2012). Trend-preserving blending of passive and active microwave soil moisture retrievals. *Remote Sensing of Environment*, 123, 280–297.

Liu, Y. Y., Parinussa, R. M., Dorigo, W. A., De Jeu, R. A. M., Wagner, W., Van Dijk, A. I. J. M., McCabe, M. F., & Evans, J. P. (2011). Developing an improved soil moisture dataset by blending passive and active microwave satellite-based retrievals. *Hydrology and Earth System Sciences*, 15, 425–436, doi:10.5194/hess-15-425-2011.

Liu, J.-G. & Xie, Z.-H. (2013). Improving simulation of soil moisture in China using a multiple meteorological forcing ensemble approach. *Hydrology and Earth System Sciences*, 17, 3355–3369.

Loew, A. (2008). Impact of surface heterogeneity on surface soil moisture retrievals from passive microwave data at the regional scale: The Upper Danube case. *Remote Sensing of Environment*, 112(1), 231-248.

Loew, A., Holmes, T., & De Jeu, R. (2009). The European heat wave 2003: Early indicators from multisensoral microwave remote sensing? *Journal of Geophysical Research*, 114, D05103, doi:10.1029/2008JD010533.

Meesters, A. C. A., De Jeu, R. A. M., & Owe, M. (2005). Analytical derivation of the vegetation optical depth from the microwave polarization difference index. *IEEE Geoscience and Remote Sensing Letters*, 2(2), 121–123.

Naeimi, V., Scipal, K., Bartalis, Z., Hasenauer, S., & Wagner, W. (2009). An improved soil moisture retrieval algorithm for ERS and METOP scatterometer observations. *IEEE Transactions on Geoscience and Remote Sensing*, 47, 1999–2013.

Naeimi. V., & Wagner. W. (2010). C-band Scatterometers and Their Applications, Geoscience and Remote Sensing New Achievements, Pasquale Imperatore and Daniele Riccio (Ed.), ISBN: 978-953-7619-97-8, InTech, http://www.intechopen.com/books/geoscience-and-remote-sensing-newachievements/c band-scatterometers-and-their-applications

Njoku, E. (2010). updated daily. AMSR-E/Aqua daily L3 surface soil moisture, interpretive parameters, & QC ease-grids V006, [January 2007–December 2008]. Boulder, Colorado USA: National Snow and Ice Data Center. Digital media.

Njoku, E., Ashcroft, P., Chan, T., & Li, L. (2005). Global survey of statistics of radiofrequency interference in AMSR–E land observations. *IEEE Transactions on Geoscience and Remote Sensing*, 43, 938−947.

Njoku, E. G., & Entekhabi, D. (1996). Passive microwave remote sensing of soil moisture. *Journal of Hydrology*, 184, 101–129.

Njoku, E. G., Jackson, T. J., Lakshmi, V., Chan, T. K., & Nghiem, S. V. (2003). Soil moisture retrieval from AMSR-E. *IEEE Transactions on Geoscience and Remote Sensing*. 41, 215–229.

Njoku, E. G., Wilson, W. J., Yueh, S. H., Dinardo, S. J., Li, F. K., Jackson, T. J., Lakshmi, V., & Bolten, J. (2002). Observations of Soil Moisture Using a Passive and Active Low-Frequency Microwave Airborne Sensor During SGP99. *IEEE Transactions on Geoscience and Remote Sensing*. 40(12), 2659–2673.

Owe, M., De Jeu, R. A. M., & Holmes, T. R. H. (2008). Multi-sensor historical climatology of satellite derived global land surface moisture. *Journal of Geophysical Research*, 113(F1 F01002). doi:10.1029/2007JF000769.

Owe, M., De Jeu, R. A. M., & Walker, J. P. (2001). A methodology for surface soil moisture and vegetation optical depth retrieval using the microwave polarization difference index. *IEEE Transactions on Geoscience and Remote Sensing*, 39(8), 1643–1654.

Parrens, M., Zakharova, E., Lafont, S., Calvet, J. -C., Kerr, Y., Wagner, W., et al. (2012). Comparing soil moisture retrievals from SMOS and ASCAT over France. *Hydrology and Earth System Sciences*, 16, 423–440.

Paulik, C., Dorigo, W., Wagner, W., Kidd, R. (2014). Validation of the ASCAT Soil Water Index using in situ data from the International Soil Moisture Network. *International Journal of Applied Earth Observation and Geoinformation*, 30, 1-8.

Rawls, W., Brakensiek, D., & Miller, N. (1983). Green-Ampt Infiltration Parameters from Soils Data. *Journal of Hydraulic Engineering*. 109(1), 62–70.

Reichle, R. H., & Koster, R. D. (2004). Bias reduction in short records of satellite soil moisture, *Geophysical Research Letters*. 31, L19501. doi:10.1029/2004GL020938.

Rudiger, C., Calvet, J. C., Gruhier, C., Holmes, T. R. H., De Jeu, R. A. M., & Wagner, W. (2009). An intercomparison of ERS-Scat and AMSR-E soil moisture observations with model simulations over France. Journal of Hydrometeorolgy, 10(2), 431–447, doi:10.1175/2008JHM997.1.

Schmugge, T. J., Kustas, W. P., Ritchie, J. C., Jackson, T. J., & Rango, A. (2002). Remote sensing in hydrology. *Advanced Water Resources*. 25, 1367–1385.

Scipal, K., Drusch, M., & Wagner, W. (2008). Assimilation of a ERS scatterometer derived soil moisture index in the ECMWF numerical weather prediction system, *Advanced Water Resources*. 31, 1101-1112.

Su, C.-H., Ryu, D., Young, R., Western, A., & W. Wagner, W. (2013). Intercomparison of microwave satellite soil moisture retrievals over the Murrumbidgee Basin, southeast Australia, *Remote Sensing of Environment*, 134, 1–11.

Sur, C., Jung, Y, Choi, M. (2013). Temporal stability and variability of field scale soil moisture on mountainous hillslopes in Northeast Asia. *Geoderma*. 207–208, 234–243. doi:10.1016/j.geoderma.2013.05.007.

Taylor, K. E. (2001). Summarizing multiple aspects of model performance in a single diagram. *Journal of Geophysical Research*, 106, 7183–7192.

Van de Griend, A. A., Wigneron, J. P., & Waldteufel, P. (2003). Consequences of surface heterogeneity for parameter retrieval from 1.4-GHz multiangle SMOS observations. *IEEE Transactions on Geoscience and Remote Sensing*, 41(4), 803.

Veldkamp, E., & O'Brien, J. J. (2000). Calibration of a frequency domain reflectometry sensor for humid tropical soils of volcanic origin. Soil Science Society America Journal, 64 (5), 1549–1553.

Verspeek, J., Stoffelen, A., Portabella, M., Bonekamp, H., Anderson, C., & Saldana, J. F. (2010). Validation and calibration of ASCAT using CMOD5.n. *IEEE Transactions on Geoscience and Remote Sensing*, 48(1), 386−395.

Wagner, W., Hahn, S., Kidd, R., Melzer, T., Bartalis, Z., Hasenauer, S., et al. (2013). The ASCAT soil moisture product: Specifications, validation, results, and emerging applications. *Meteorologische Zeitschrift*, 22(1), 5–33. DOI 10.1127/0941-2948/2013/0399.

Wagner, W., Naeimi, V., Scipal, K., De Jeu, R., & Martinez-Fernandez, J. (2007). Soil moisture from operational meteorological satellites. *Hydrogeology Journal*, 15, 121–131.

Wagner, W., Lemoine, G., Borgeaud, M., & Rott, H. (1999). A study of vegetation cover effects on ERS scatterometer data. *IEEE Transactions on Geoscience and Remote Sensing*, 37(2), 938-948.

Wagner, W., Lemoine, G., & Rott, H. (1999). A method for estimating soil moisture from ERS scatterometer and soil data. *Remote Sensing of Environment*, 70, 191–207.

Western, A.W., Grayson, R.B., Blöschl, G. (2002). Scaling of soil moisture: A hydrologic perspective. *Annual Review of Earth and Planetary Sciences*, 30, 149–180. doi:10.1146/annurev.earth.30.091201.140434

WMO (2010). Implementation plan for the global observing system for climate in support of the UNFCCC (2010 update). *World Meteorological Organization*. GCOS-138.

WMO (2013). WMO statement on the status of the global climate in 2012. *World Meteorological Organization*. WMO_No. 1108.

Yilmaz, M. T., Crow, W. T., Anderson, M. C., & Hain, C. (2012). An objective methodology for merging satellite- and model-based soil moisture products. *Water Resources Research*, 48, W11502.

Zhang, A., & Jia, G. (2013). Monitoringmeteorological drought in semiarid regions using multi-sensormicrowave remote sensing data. *Remote Sensing of Environment*, 134, 12–23.

Table 1 The characteristics of study areas.

Area	Latitude (degree)	Longitude (degree)	Elevation (m a.s.l)	Annual rainfall (mm)	Temperature (℃)	Relative humidity (%)	Soil texture	Land use
Suwon	37° 16´ N	126° 59´ E	143 m	1470.6 mm	12.3 ℃	73.5 %	Sandy loam	Urban
Seosan	36° 46´ N	126° 29´ E	30 m	2141.8 mm	11.7 ℃	73.8 %	Loam	Cropland
Jeonju	35° 49´ N	127° 09´ E	53 m	1867.5 mm	13.6 ℃	66.0 %	Loam	Urban
Cheorwon	38° 08´ N	127° 18´ E	156 m	1581.4 mm	10.1 ℃	71.8 %	Sandy loam	Cropland
Chuncheon	37° 54´ N	127° 44´ E	79 m	1464.0 mm	11.0 ℃	70.0 %	Silt loam	Urban
Andong	36° 34´ N	128° 42´ N	140 m	1073.8 mm	12.3 ℃	66.6 %	Sandy loam	Grassland
Cheongju	36° 38´ N	127° 26´ N	58 m	1422.4 mm	13.1 ℃	65.3 %	Loam	Urban
Jinju	35° 09´ N	128° 02´ N	29 m	1896.0 mm	13.2 ℃	67.5 %	Loamy sand	Mixed forest
Seolmacheon	37° 56´ N	126° 57´ E	269 m	1827.2 mm	10.4 ℃	73.6 %	Sandy loam	Mixed forest

Table 2 Specifications of the five datasets used in this study.

	FDR (In-situ)	**AMSR-E (NSIDC)**	**AMSR-E (VUA-NASA)**	**AMSR-E (USDA)**	**ASCAT (TU-WIEN)**
Observation period	Jan. 2008 ~ Dec. 2010	Jun. 2002 ~ Dec. 2010	Jun. 2002 ~ Oct. 2010	Jun. 2002 ~ Dec. 2010	Jan. 2007 ~
Spatial Resolution (grid)	Point	38 (25 km)	25 km	25 km	25 km (12.5 km)
Measurement interval	Hourly	Daily	Daily	Daily	Daily
Overpass time (A , D)	-	13:30, 1:30	13:30, 1:30	13:30	11:30, 23:30
Penetration depth (sample size*)	10, 20, 30, 50 cm (3672)	Surface (226) Root zone (306)	Surface (214)	Root zone (304)	Surface (278) Root zone (304)

The sample size* is the mean at each site from the ascending and descending pass.

Table 3 Statistics of AMSR-E SSM for the NSIDC and VUA-NASA products with in-situ data at 10cm depth.

Area (10 cm)	NSIDC SSM (m^3/m^3)					VUA-NASA SSM (m^3/m^3)				
	Average	**Stdev**	**R**	**Bias**	**RMSE**	**Average**	**Stdev**	**R**	**Bias**	**RMSE**
Suwon	0.12	0.02	0.37**	-0.09	0.09	0.40	0.08	0.43**	0.18	0.20
Seosan	0.09	0.02	0.23**	-0.03	0.06	0.33	0.07	0.60**	0.19	0.20
Jeonju	0.14	0.02	0.61**	-0.07	0.07	0.39	0.08	0.31**	0.18	0.19
Cheorwon	0.13	0.01	0.57**	-0.08	0.09	0.35	0.11	0.43**	0.13	0.17
Chuncheon	0.13	0.01	0.54**	0.00	0.02	0.39	0.13	0.19*	0.26	0.29
Cheongju	0.13	0.01	0.13*	-0.14	0.16	0.37	0.08	0.56**	0.10	0.13
Jinju	0.13	0.02	0.41**	0.02	0.05	0.38	0.11	0.27**	0.26	0.27
Andong	0.14	0.02	0.11	0.00	0.06	0.40	0.13	0.43**	0.27	0.29
Seolmacheon	0.12	0.01	0.52**	-0.09	0.11	0.44	0.11	0.58**	0.22	0.24
Average	***0.13***	***0.01***	***0.39***	***-0.05***	***0.08***	***0.38***	***0.10***	***0.42***	***0.20***	***0.22***

* and ** indicates significance at the 0.05 and 0.01 probability level, respectively.

Table 4 Statistics of the VUA AMSR-E data from C- and X-band for according to overpass time (descending / ascending).

Area	**C-band** (m^3/m^3)						**X-band** (m^3/m^3)					
	Ascending			**Descending**			**Ascending**			**Descending**		
	R	**Bias**	**RMSE**	**R**	**Bias**	**RMSE**	**R**	**Bias**	**RMSE**	**R**	**Bias**	**RMSE**
Suwon	0.43**	0.18	0.20	0.24*	0.21	0.24	0.36*	0.16	0.20	0.10	0.26	0.27
Seosan	0.60**	0.19	0.20	0.29**	0.23	0.24	0.32**	0.18	0.22	0.21*	0.26	0.27
Jeonju	0.31**	0.18	0.19	0.12	0.28	0.31	0.29**	0.12	0.15	0.07	0.23	0.26
Cheorwon	0.43**	0.13	0.17	0.19*	0.27	0.30	0.42**	0.16	0.20	0.13	0.30	0.33
Chuncheon	0.19*	0.26	0.29	0.05	0.33	0.36	0.13	0.25	0.31	0.07	0.35	0.38
Cheongju	0.56**	0.10	0.13	0.31**	0.14	0.18	0.43**	0.07	0.12	0.29**	0.19	0.21
Jinju	0.27**	0.26	0.27	0.04	0.34	0.35	0.24*	0.27	0.30	0.09	0.34	0.37
Andong	0.43**	0.27	0.29	0.11	0.35	0.41	0.24*	0.08	0.14	0.11	0.17	0.21
Seolmacheon	0.58**	0.22	0.24	0.31**	0.27	0.28	0.49**	0.19	0.24	0.27**	0.27	0.29
Average	**0.42**	**0.20**	0.**22**	**0.17**	0.**27**	0.**30**	**0.29**	**0.17**	**0.21**	**0.09**	**0.26**	**0.29**

* and ** indicates significance at the 0.05 and 0.01 probability level, respectively.

Table 5 Statistics of AMSR-E RZSM for the NSIDC SWI and USDA RZSM products with in-situ data at 20cm depth.

Area (20 cm)	**NSIDC SWI** (m^3/m^3)					**USDA RZSM** (m^3/m^3)				
	Average	**Stdev**	**R**	**Bias**	**RMSE**	**Average**	**Stdev**	**R**	**Bias**	**RMSE**
Suwon	0.12	0.01	0.35**	-0.19	0.20	0.49	0.04	0.70**	0.17	0.18
Seosan	0.09	0.02	0.32**	-0.08	0.09	0.47	0.05	0.47**	0.30	0.31
Jeonju	0.14	0.02	0.72**	-0.11	0.11	0.59	0.08	0.79**	0.34	0.34
Cheorwon	0.13	0.00	0.68**	-0.08	0.08	0.61	0.06	0.69**	0.40	0.41
Chuncheon	0.13	0.01	0.66**	0.01	0.02	0.47	0.06	0.70**	0.34	0.35
Cheongju	0.13	0.01	0.16**	0.19	0.19	0.46	0.07	0.88**	0.14	0.15
Jinju	0.13	0.01	0.66**	0.02	0.02	0.44	0.05	0.82**	0.32	0.33
Andong	0.14	0.01	0.18**	-0.04	0.06	0.40	0.10	0.74**	0.22	0.24
Average	***0.13***	***0.01***	***0.47***	***-0.04***	***0.10***	***0.49***	***0.06***	***0.72***	***0.28***	***0.29***

* and ** indicates significance at the 0.05 and 0.01 probability level, respectively.

Table 6

Comparison between (a) *in-situ* data at 10 cm depth and the rescaled ASCAT SSM products from May 1 to September 30.

Area	*In-situ* (m^3/m^3)		*rescaled* ASCAT Surface Soil Moisture (m^3/m^3)				
	Average	**Stdev**	**Average**	**Stdev**	**R**	**Bias**	**RMSE**
Suwon	0.21	0.03	0.19	0.07	0.64**	0.02	0.06
Seosan	0.13	0.05	0.14	0.08	0.62**	0.01	0.06
Jeonju	0.21	0.03	0.19	0.08	0.54**	-0.02	0.07
Cheorwon	0.21	0.04	0.30	0.05	0.51**	0.09	0.10
Chuncheon	0.12	0.03	0.34	0.06	0.48**	0.21	0.22
Cheongju	0.26	0.08	0.21	0.07	0.41**	-0.05	0.09
Jinju	0.11	0.05	0.20	0.07	0.44**	0.08	0.11
Andong	0.13	0.06	0.28	0.05	0.42**	0.15	0.16
Seolmacheon	0.22	0.05	0.25	0.06	0.70**	0.03	0.06
Average	***0.18***	***0.05***	***0.23***	***0.07***	***0.53***	***0.06***	***0.10***

* and ** indicates significance at the 0.05 and 0.01 probability level, respectively.

Table 7

Comparison between *in-situ* data at 20 cm depth and the rescaled ASCAT SWI products (T=5) from May 1 to September 30.

Area	***In-situ*** (m^3/m^3)		***rescaled*** **ASCAT Soil Water Index** (m^3/m^3)				
	Average	**Stdev**	**Average**	**Stdev**	**R**	**Bias**	**RMSE**
Suwon	0.31	0.01	0.24	0.04	0.73**	-0.08	0.08
Seosan	0.17	0.05	0.17	0.06	0.51**	0.00	0.05
Jeonju	0.25	0.03	0.22	0.05	0.77**	-0.03	0.04
Cheorwon	0.21	0.03	0.35	0.03	0.80**	0.14	0.14
Chuncheon	0.14	0.02	0.35	0.03	0.85**	0.21	0.21
Cheongju	0.32	0.04	0.24	0.04	0.80**	-0.07	0.08
Jinju	0.12	0.02	0.23	0.05	0.84**	0.12	0.12
Andong	0.18	0.05	0.32	0.03	0.67**	0.12	0.13
Average	***0.21***	***0.03***	***0.27***	***0.04***	***0.75***	***0.06***	***0.11***

* and ** indicates significance at the 0.05 and 0.01 probability level, respectively.

Table 8

Correlations of root zone soil moisture between ground based measurements (10, 20, 30, and 50 cm) and USDA AMSR-E and ASCAT satellite products.

	USDA AMSR-E	**ASCAT soil water index**				
		T=1	T=5	T=10	T=15	T=20
10 cm						
Suwon	0.62**	0.81**	0.66**	0.58**	0.53**	0.49**
Seosan	0.50**	0.70**	0.53**	0.44**	0.38**	0.34**
Jeonju	0.82**	0.75**	0.82**	0.80**	0.76**	0.72**
Cheorwon	0.67**	0.79**	0.77**	0.71**	0.66**	0.63**
Chuncheon	0.73**	0.74**	0.84**	0.85**	0.83**	0.81**
Cheongju	0.83**	0.68**	0.82**	0.84**	0.83**	0.81**
Jinju	0.79**	0.82**	0.81**	0.74**	0.70**	0.66**
Andong	0.71**	0.59**	0.65**	0.62**	0.60**	0.58**
Seolmacheon	0.61**	0.86**	0.83**	0.72**	0.66**	0.62**
Average	**0.70**	**0.75**	**0.75**	**0.70**	**0.66**	**0.63**
20 cm						
Suwon	0.70**	0.81**	0.73**	0.63**	0.57**	0.53**
Seosan	0.47**	0.66**	0.51**	0.43**	0.38**	0.33**
Jeonju	0.79**	0.71**	0.77**	0.75**	0.71**	0.67**
Cheorwon	0.69**	0.76**	0.80**	0.76**	0.72**	0.69**
Chuncheon	0.70**	0.72**	0.85**	0.87**	0.86**	0.85**
Cheongju	0.88**	0.62**	0.80**	0.84**	0.83**	0.81**
Jinju	0.82**	0.77**	0.84**	0.82**	0.79**	0.77**
Andong	0.74**	0.58**	0.67**	0.66**	0.65**	0.64**
Average	**0.72**	**0.70**	**0.75**	**0.72**	**0.69**	**0.66**
30 cm						
Suwon	0.70**	0.82**	0.70**	0.58**	0.52**	0.47**
Seosan	0.37**	0.53**	0.36**	0.30**	0.27**	0.24**
Jeonju	0.64**	0.68**	0.65**	0.61**	0.56**	0.52**
Cheorwon	0.63**	0.62**	0.77**	0.76**	0.74**	0.72**
Chuncheon	0.51**	0.52**	0.61**	0.57**	0.53**	0.49**
Cheongju	0.80**	0.35**	0.64**	0.78**	0.83**	0.84**
Jinju	0.80**	0.71**	0.80**	0.79**	0.77**	0.75**
Andong	0.68**	0.51**	0.58**	0.60**	0.62**	0.63**
Total	**0.64**	**0.59**	**0.64**	**0.62**	**0.61**	**0.58**
50 cm						
Suwon	0.61**	0.64**	0.49**	0.37**	0.31**	0.27**
Seosan	0.45**	0.59**	0.40**	0.32**	0.28**	0.23**
Jeonju	-0.23	-0.05	-0.11	-0.12	-0.09	-0.06
Cheorwon	0.58**	0.58**	0.74**	0.76**	0.76**	0.75**
Chuncheon	0.60**	0.53**	0.74**	0.81**	0.83**	0.83**
Cheongju	0.78**	0.69**	0.79**	0.81**	0.81**	0.80**
Jinju	0.71**	0.69**	0.71**	0.69**	0.66**	0.64**
Andong	0.66**	0.37**	0.49**	0.57**	0.64**	0.67**
Average	**0.52**	**0.51**	**0.53**	**0.53**	**0.53**	**0.52**

* and ** indicates significance at the 0.05 and 0.01 probability level, respectively.

Figure 1. Korea Meteorological Organization (KMO) and Seolmacheon validation sites in Korean peninsula (each star mark indicates location of the sites).

Figure 2. Temporal patterns of (a) surface soil moisture (SSM) and (b) root zone soil moisture (RZSM) through AMSR-E, ASCAT and in situ soil moisture from 1 May to 30 September 2010 at the nine sites in northeast Asia.

Figure 3. Comparison results of surface soil moisture (SSM) retrievals of R and RMSE values at nine sites.

Figure 4. Comparison results of root zone soil moisture (RZSM) retrievals of R and RMSE values at eight sites.

Figure 5. Taylor diagram of surface soil moisture products (SSM) illustrating the statistics of comparison between according to three renormalizing methods, (a) original, (b) linear regression correction (REG), (c) average - standard-deviation ($\mu-\sigma$) and (d) cumulative distribution function (CDF).

Figure 6. Taylor diagram of root zone soil moisture products (RZSM) illustrating the statistics of comparison between according to three renormalizing methods, (a) original, (b) linear regression correction (REG), (c) average - standard-deviation ($\mu-\sigma$) and (d) cumulative distribution function (CDF).

Fig.1

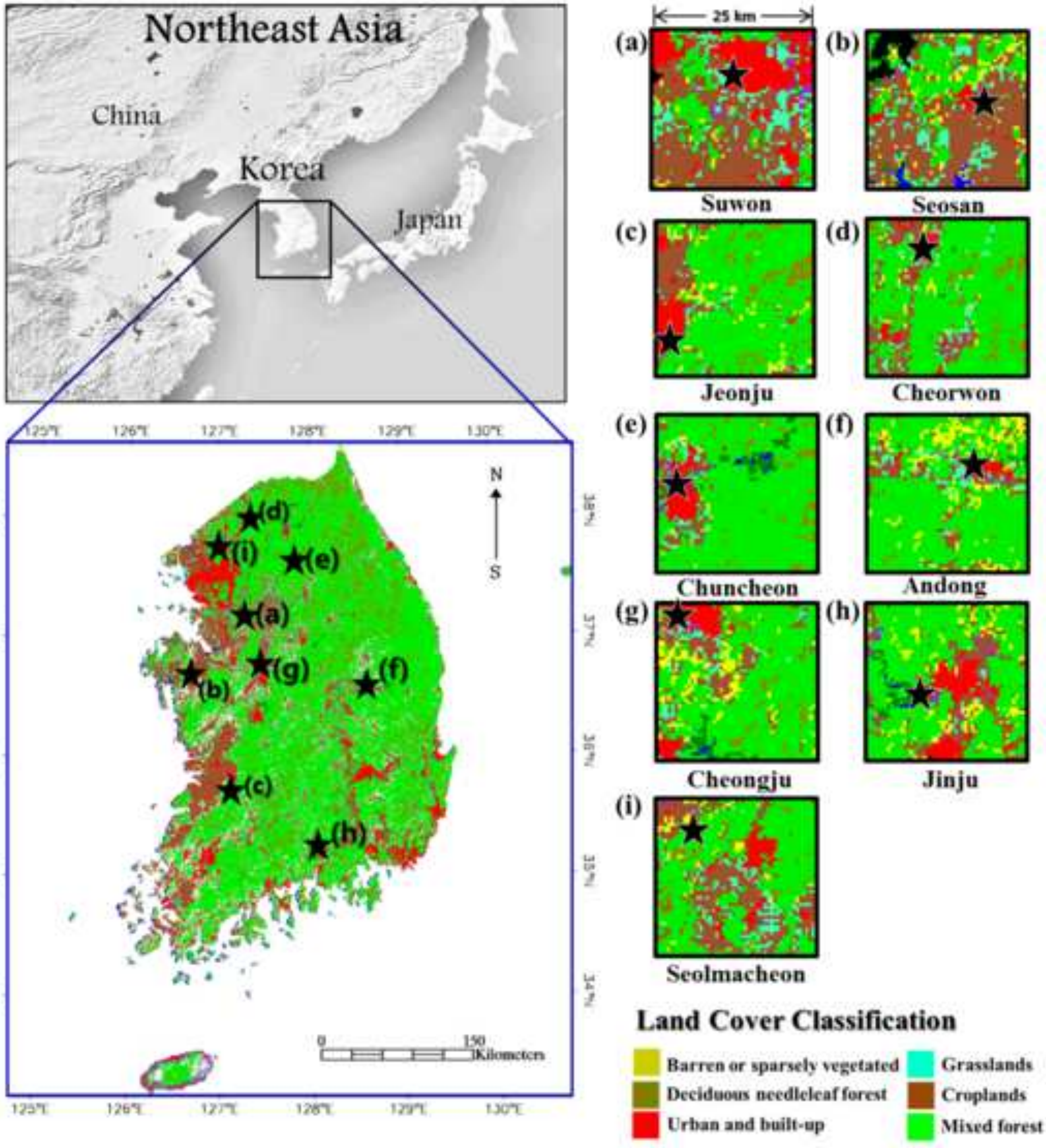

Northeast Asia
China
Korea
Japan
125°E
126°E
127°E
128°E
129°E
130°E
38°N
37°N
36°N
35°N
34°N
N
S
(a)
(b)
(c)
(d)
(e)
(f)
(g)
(h)
(i)
0
150
Kilometers
25 km
Suwon
Seosan
Jeonju
Cheorwon
Chuncheon
Andong
Cheongju
Jinju
Seolmacheon
Land Cover Classification
Barren or sparsely vegetated
Deciduous needleleaf forest
Urban and built-up
Grasslands
Croplands
Mixed forest

Fig.2a

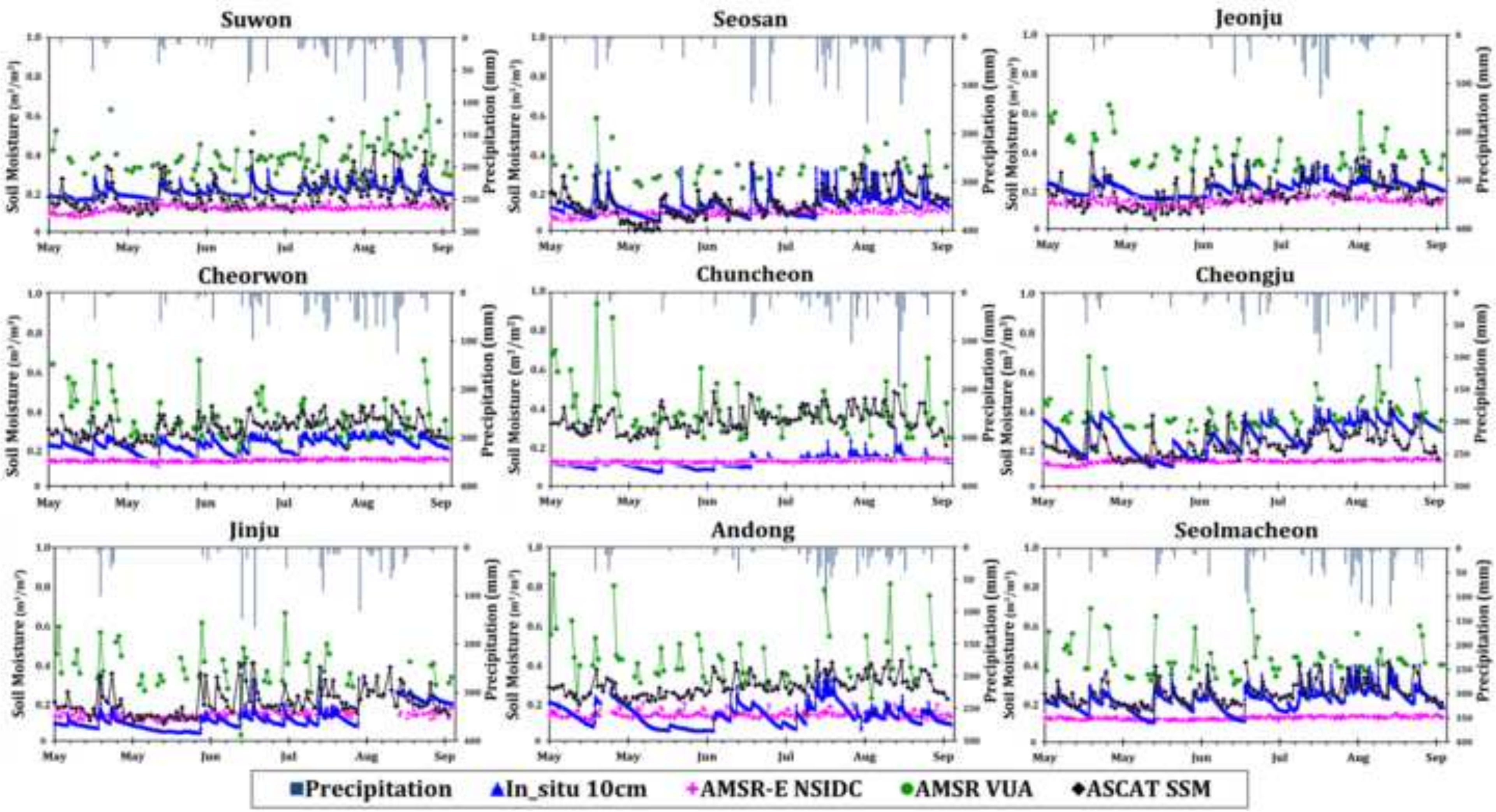
Suwon
Seosan
Jeonju
Cheorwon
Chuncheon
Cheongju
Jinju
Andong
Seolmacheon
Soil Moisture (m³/m³)
Precipitation (mm)
May
Jun
Jul
Aug
Sep
Precipitation
In_situ 10cm
AMSR-E NSIDC
AMSR VUA
ASCAT SSM

Fig.2b

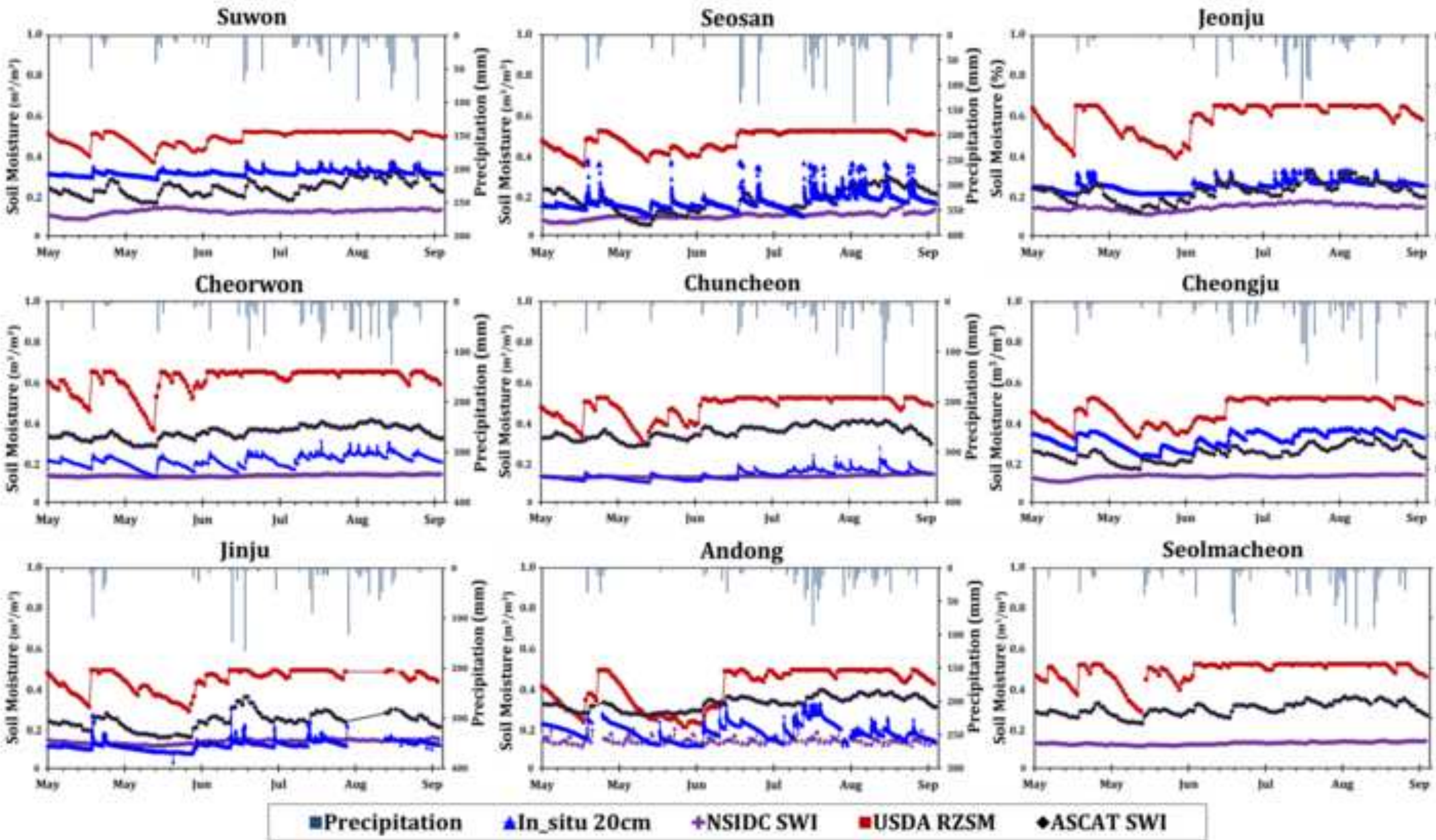
Suwon
Seosan
Jeonju
Cheorwon
Chuncheon
Cheongju
Jinju
Andong
Seolmacheon
Soil Moisture (m³/m³)
Soil Moisture (%)
Precipitation (mm)
May
May
Jun
Jul
Aug
Sep
Precipitation
In_situ 20cm
NSIDC SWI
USDA RZSM
ASCAT SWI

Fig.3a

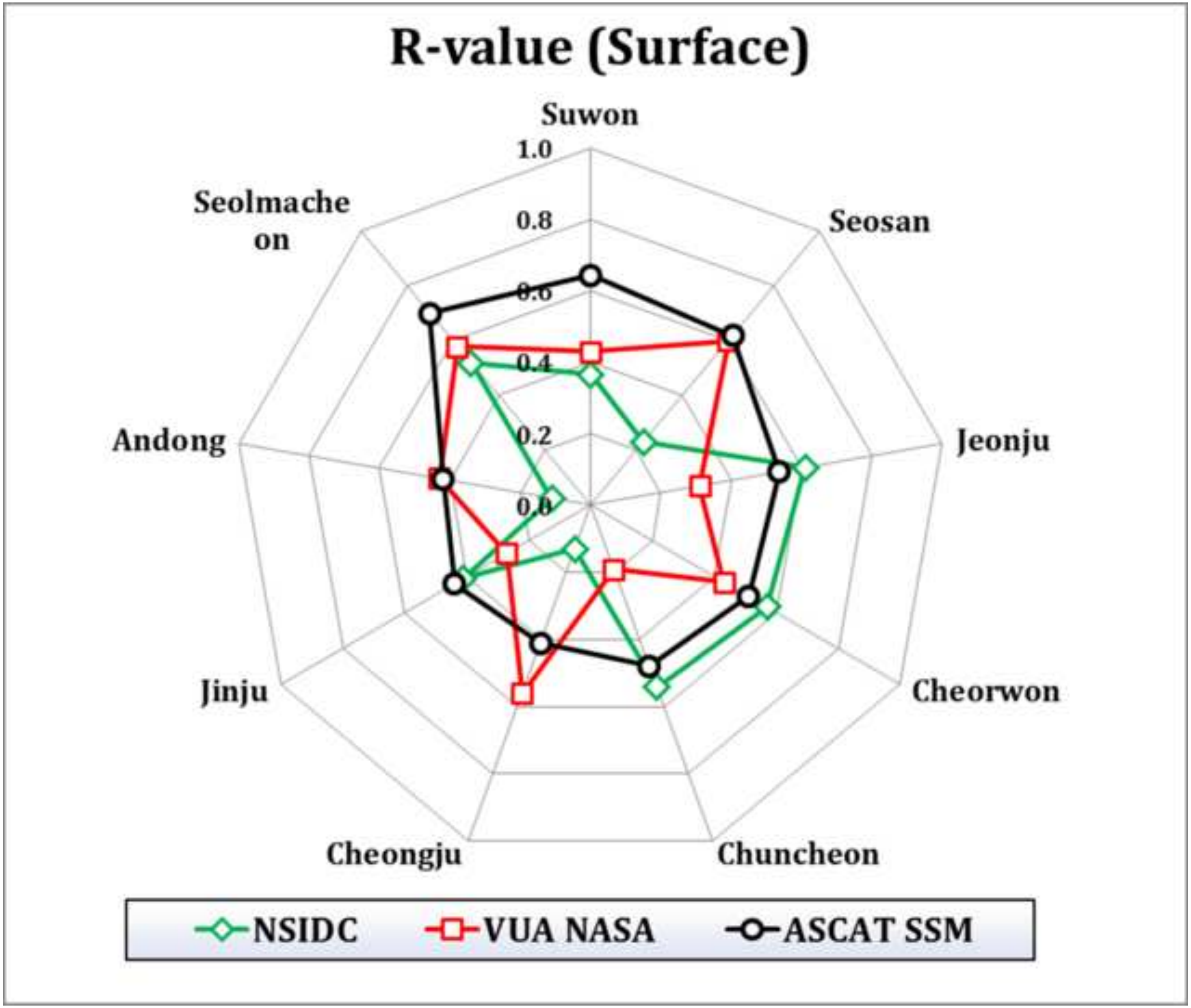
R-value (Surface)
Suwon
Seosan
Jeonju
Cheorwon
Chuncheon
Cheongju
Jinju
Andong
Seolmache
on
1.0
0.8
0.6
0.4
0.2
0.0
NSIDC
VUA NASA
ASCAT SSM

Fig.3b

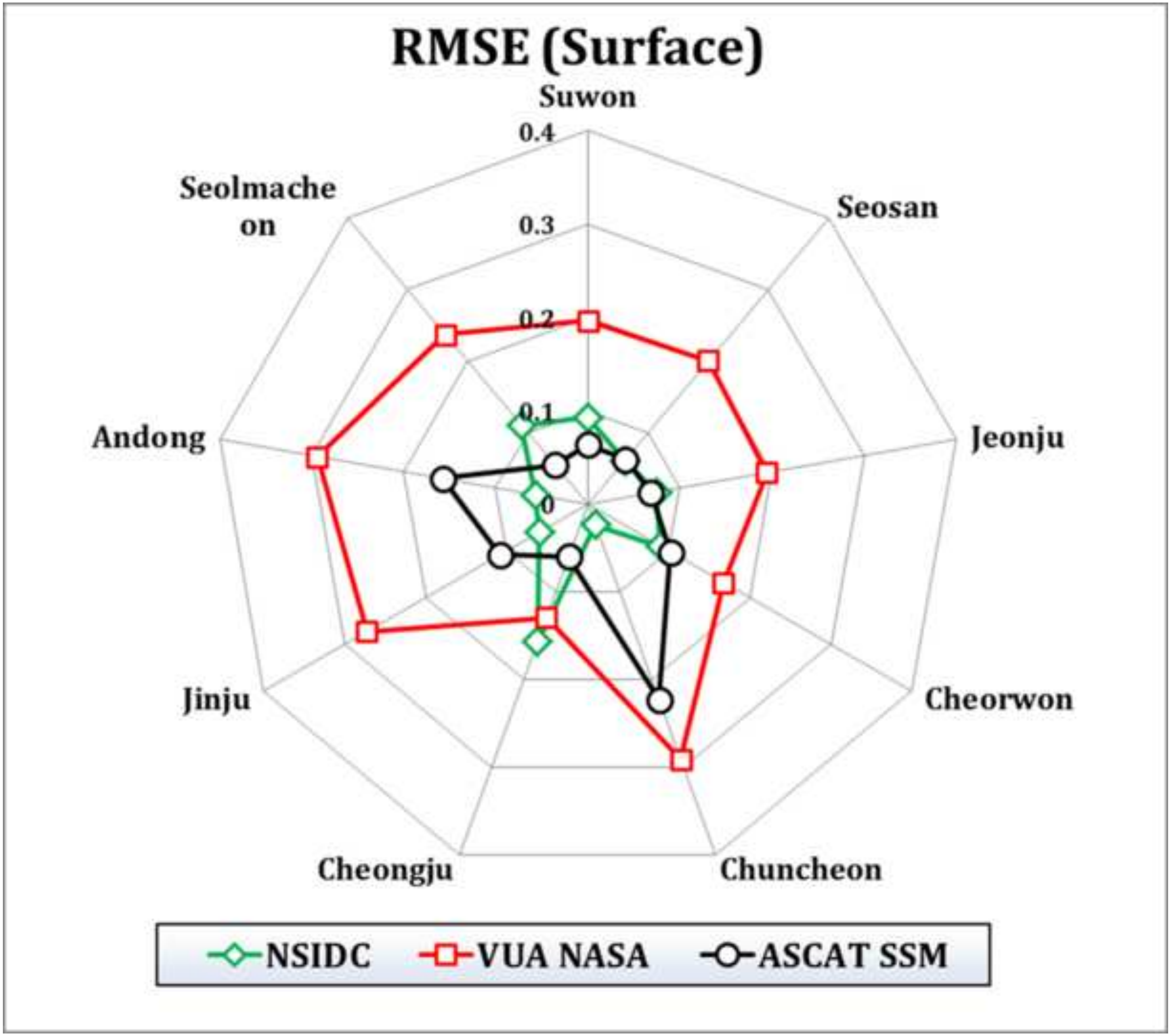
RMSE (Surface)
Suwon
Seosan
Jeonju
Cheorwon
Chuncheon
Cheongju
Jinju
Andong
Seolmacheon
0.4
0.3
0.2
0.1
0
NSIDC
VUA NASA
ASCAT SSM

Fig.4a

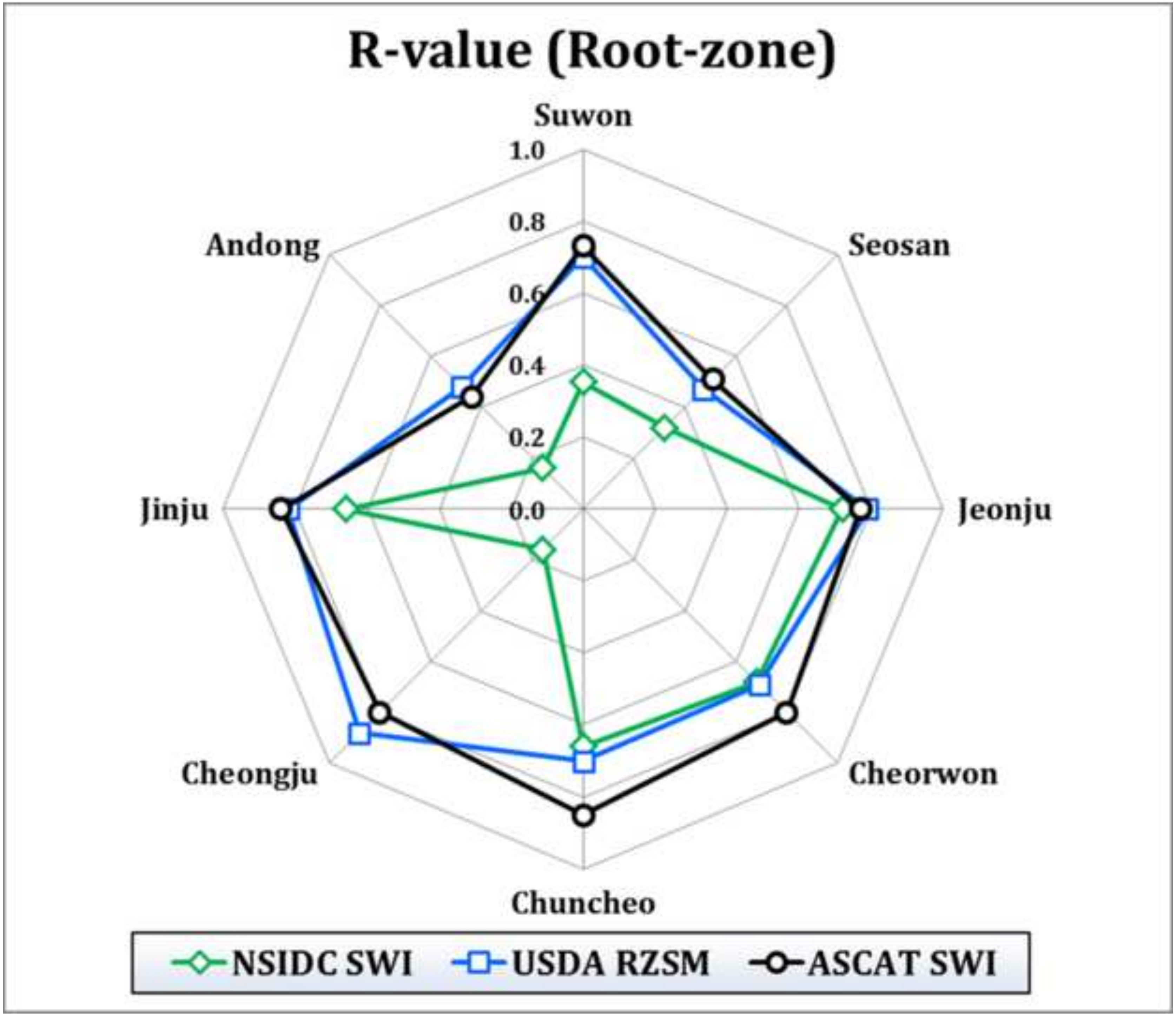

R-value (Root-zone)
Suwon
Seosan
Jeonju
Cheorwon
Chuncheo
Cheongju
Jinju
Andong
1.0
0.8
0.6
0.4
0.2
0.0
NSIDC SWI
USDA RZSM
ASCAT SWI

Fig.4b

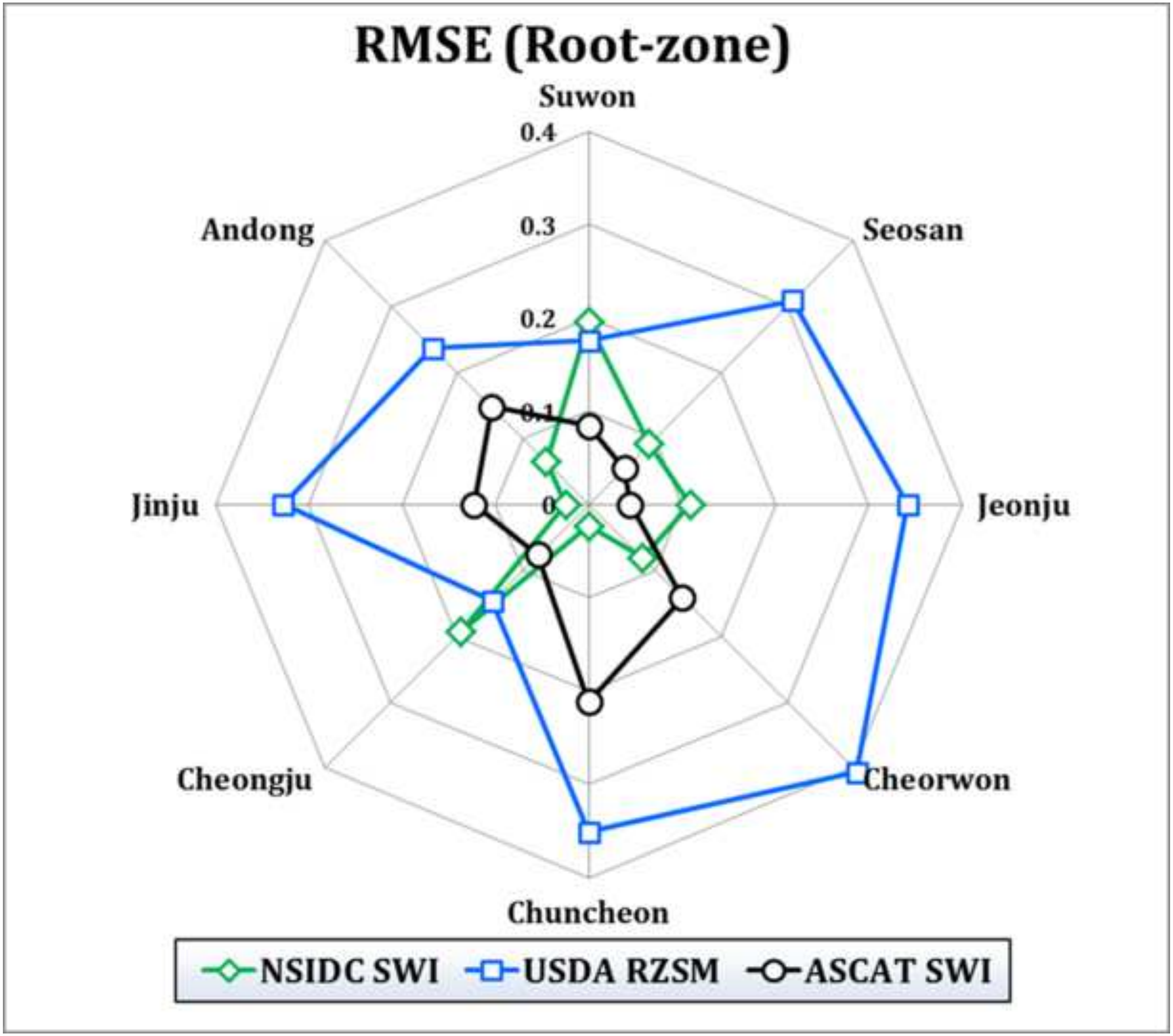
RMSE (Root-zone)
Suwon
0.4
0.3
0.2
0.1
0
Seosan
Jeonju
Cheorwon
Chuncheon
Cheongju
Jinju
Andong
NSIDC SWI
USDA RZSM
ASCAT SWI

Fig.5a

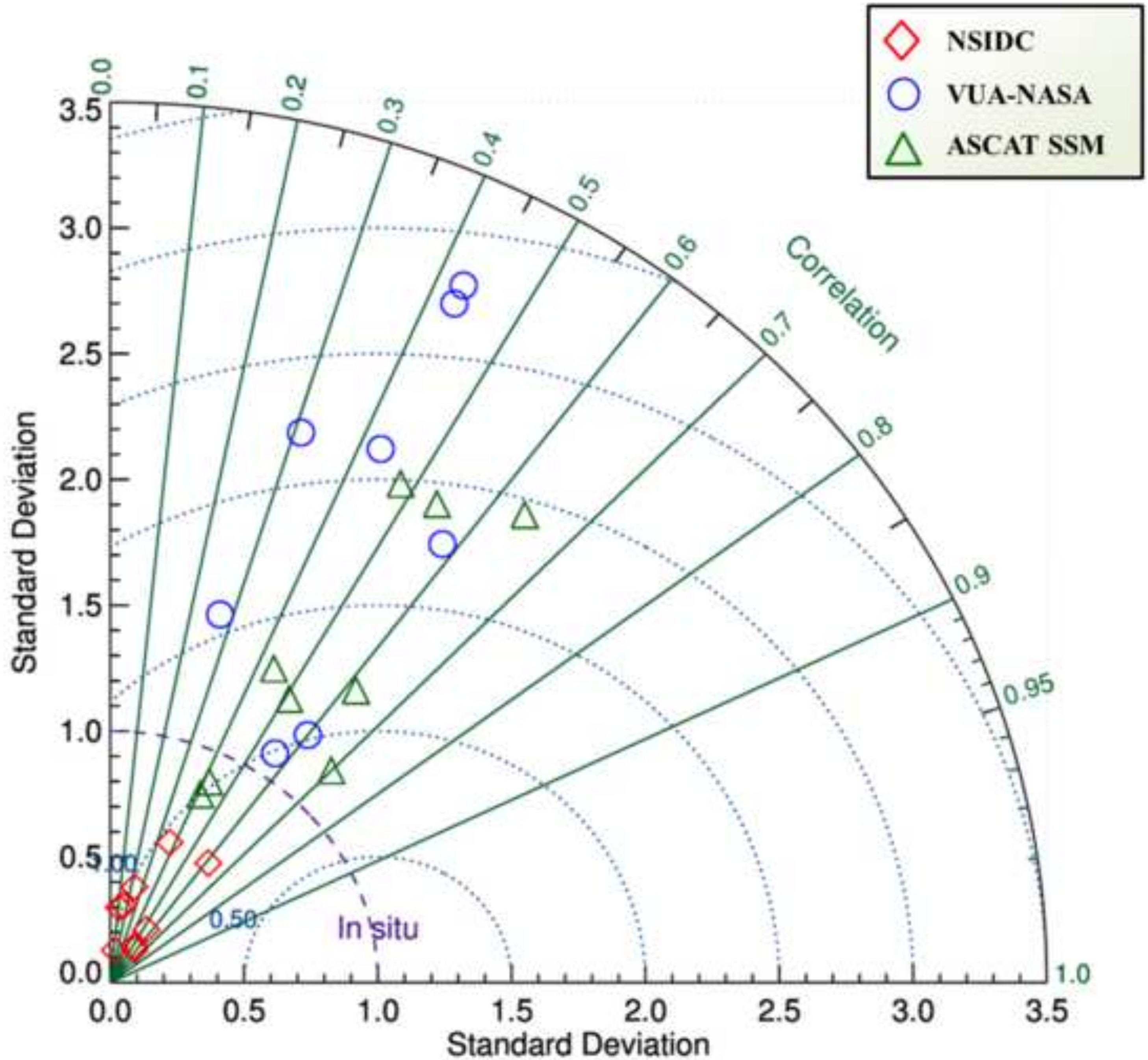

NSIDC
VUA-NASA
ASCAT SSM
Correlation
0.0
0.1
0.2
0.3
0.4
0.5
0.6
0.7
0.8
0.9
0.95
1.0
Standard Deviation
Standard Deviation
0.0
0.5
1.0
1.5
2.0
2.5
3.0
3.5
1.00
0.50
In situ

Fig.5b

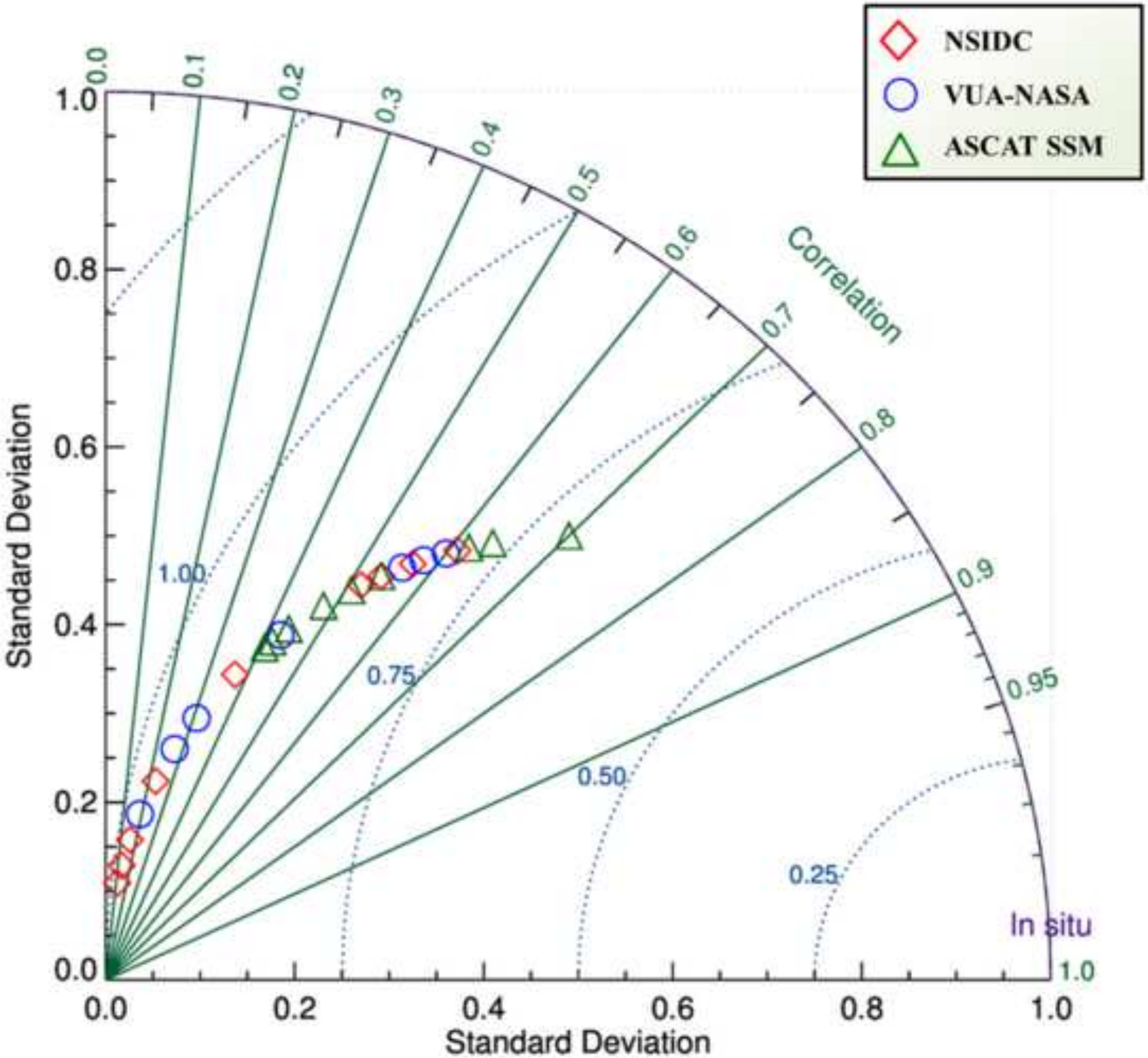
NSIDC
VUA-NASA
ASCAT SSM
Correlation
0.0
0.1
0.2
0.3
0.4
0.5
0.6
0.7
0.8
0.9
0.95
1.0
1.00
0.75
0.50
0.25
In situ
Standard Deviation
0.0
0.2
0.4
0.6
0.8
1.0
Standard Deviation

Fig.5c

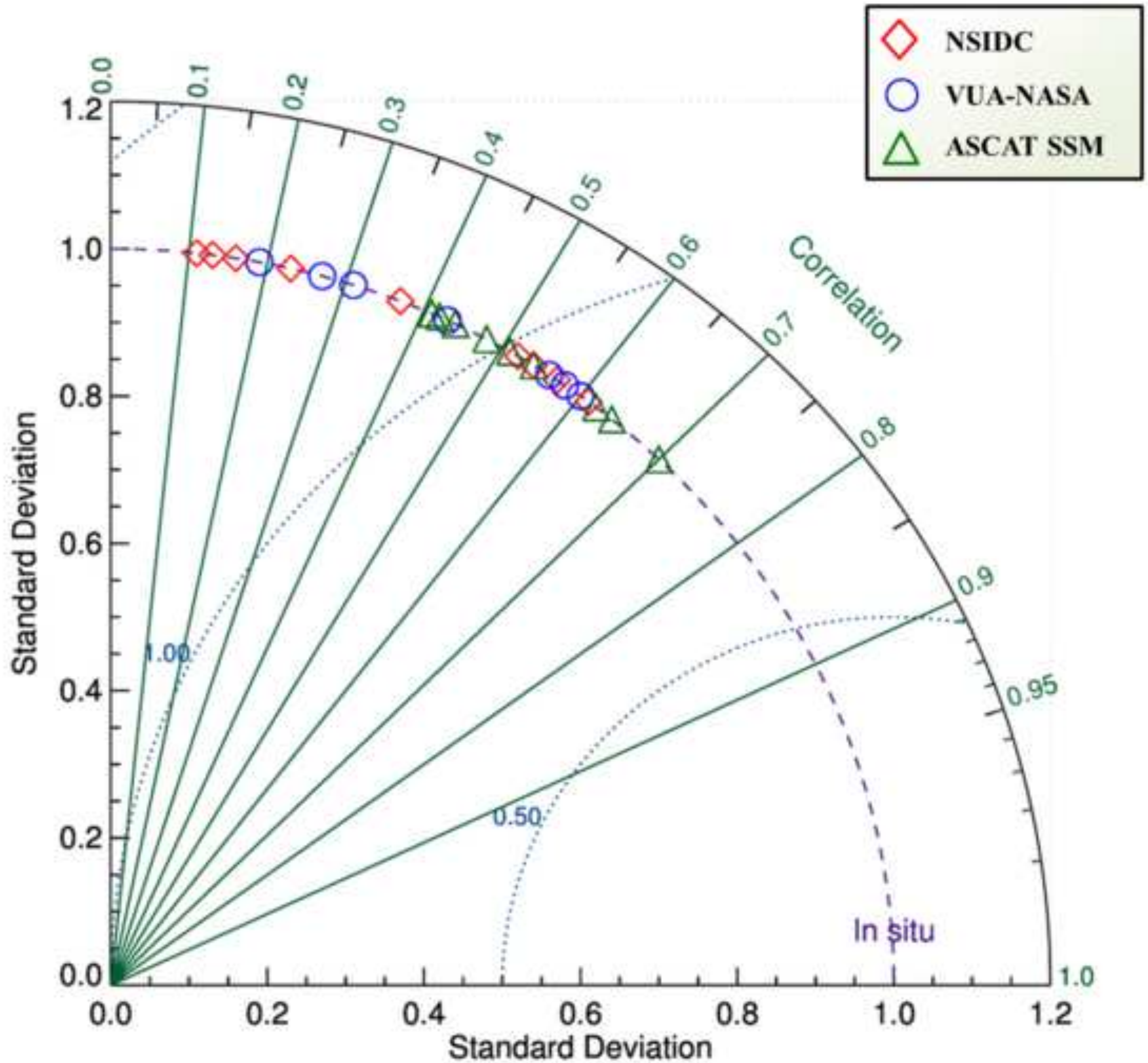

NSIDC
VUA-NASA
ASCAT SSM
Correlation
0.0
0.1
0.2
0.3
0.4
0.5
0.6
0.7
0.8
0.9
0.95
1.0
1.2
1.0
0.8
0.6
0.4
0.2
0.0
Standard Deviation
0.0
0.2
0.4
0.6
0.8
1.0
1.2
Standard Deviation
1.00
0.50
In situ

Fig.5d

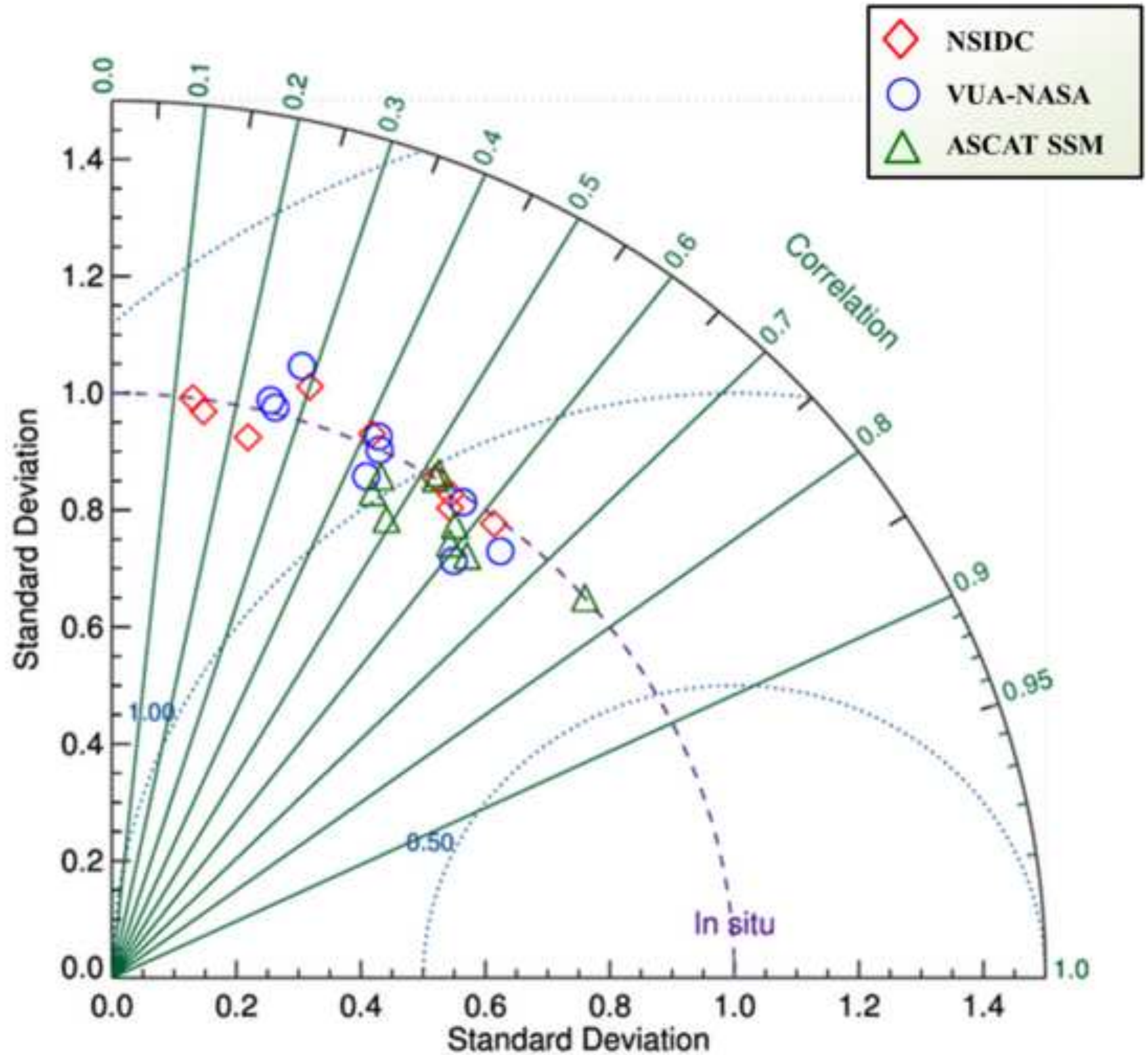

NSIDC
VUA-NASA
ASCAT SSM
Correlation
0.0
0.1
0.2
0.3
0.4
0.5
0.6
0.7
0.8
0.9
0.95
1.0
1.4
1.2
1.0
0.8
0.6
0.4
0.2
0.0
Standard Deviation
1.00
0.50
In situ
0.0
0.2
0.4
0.6
0.8
1.0
1.2
1.4
Standard Deviation

Fig.6a

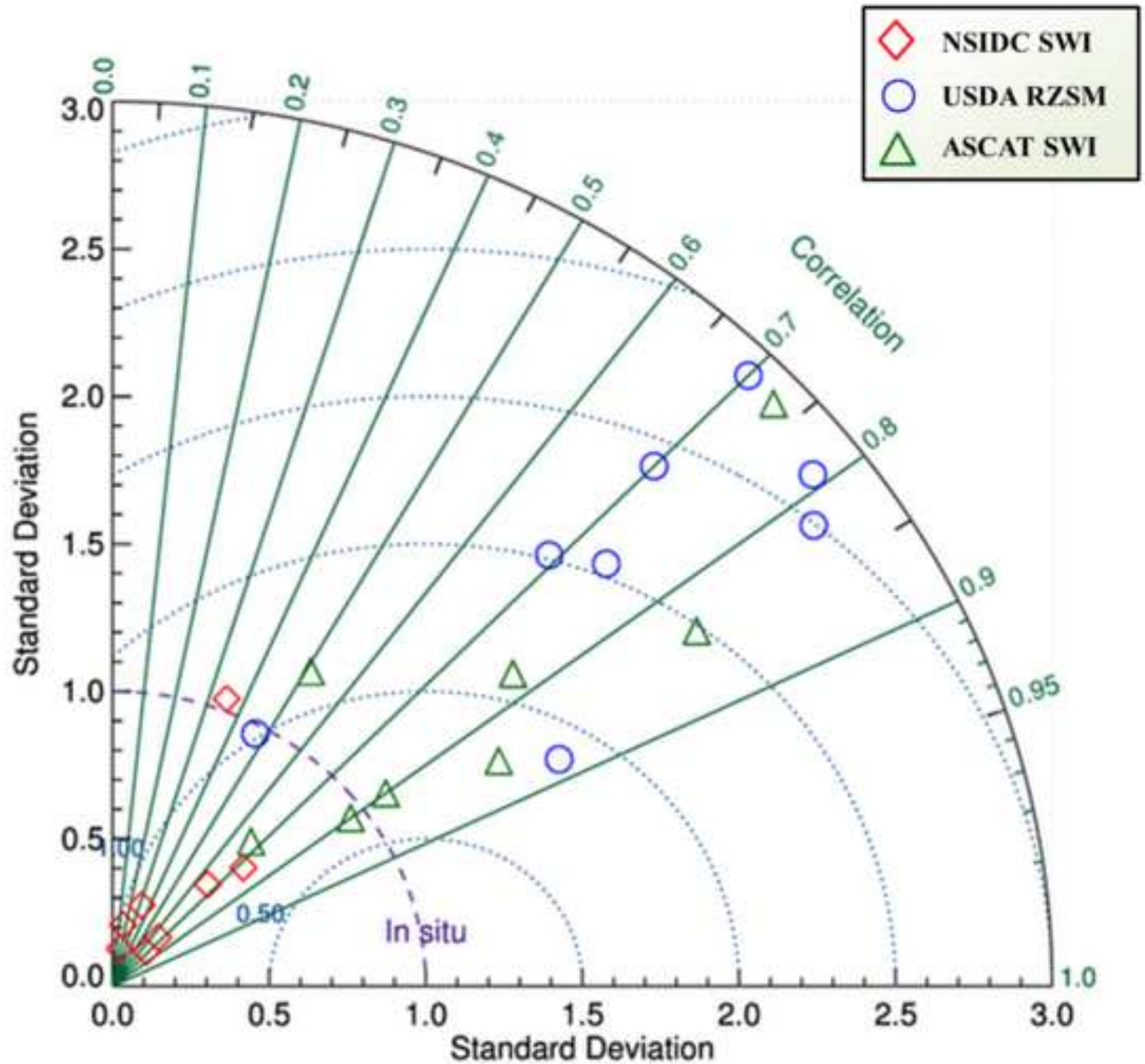
NSIDC SWI
USDA RZSM
ASCAT SWI
Correlation
Standard Deviation
Standard Deviation
In situ
0.0
0.1
0.2
0.3
0.4
0.5
0.6
0.7
0.8
0.9
0.95
1.0
0.50
1.00
0.5
1.5
2.0
2.5
3.0

Fig.6b

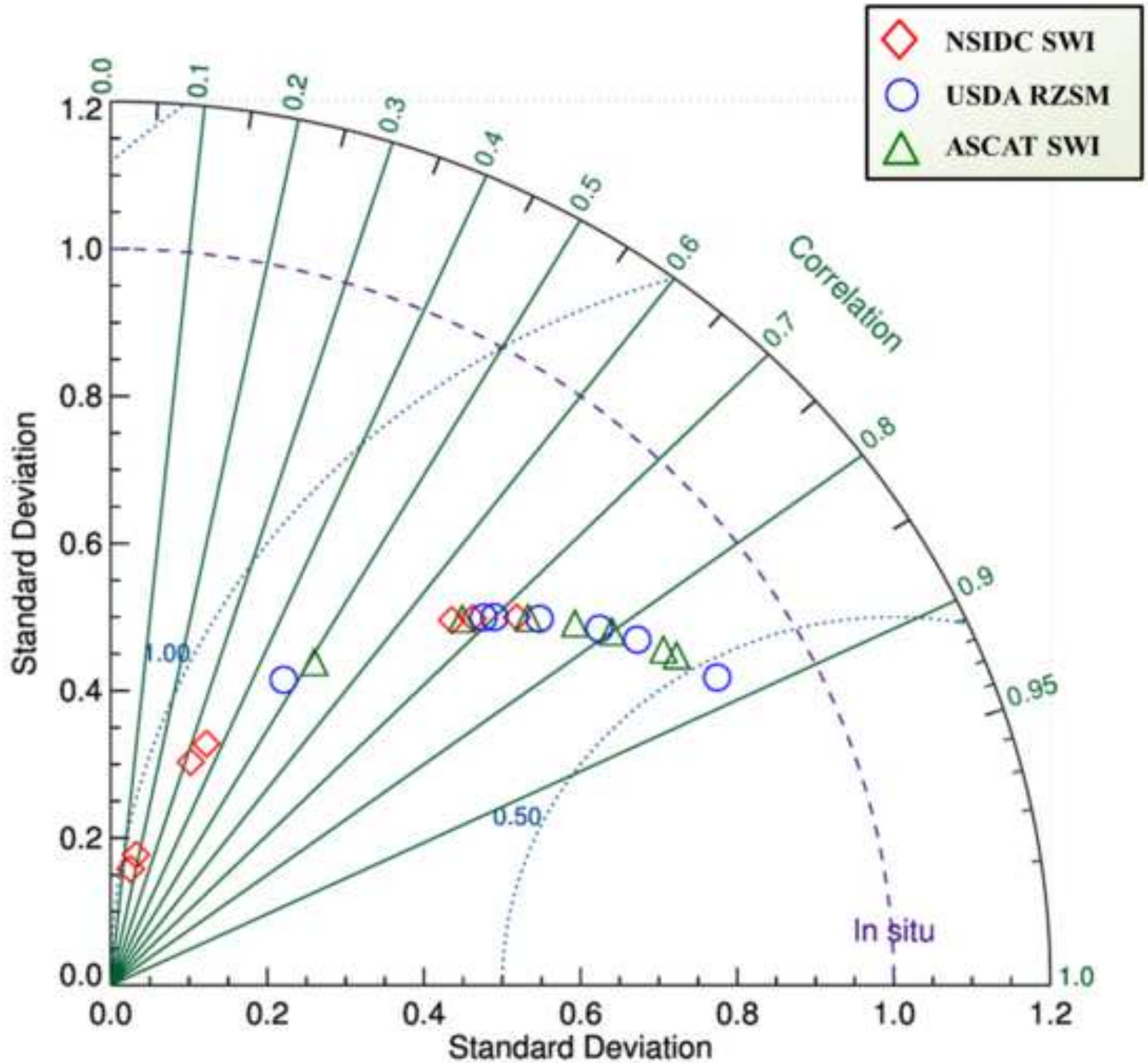
NSIDC SWI
USDA RZSM
ASCAT SWI
Correlation
Standard Deviation
Standard Deviation
In situ
1.00
0.50
0.0
0.1
0.2
0.3
0.4
0.5
0.6
0.7
0.8
0.9
0.95
1.0
0.0
0.2
0.4
0.6
0.8
1.0
1.2

Fig.6c

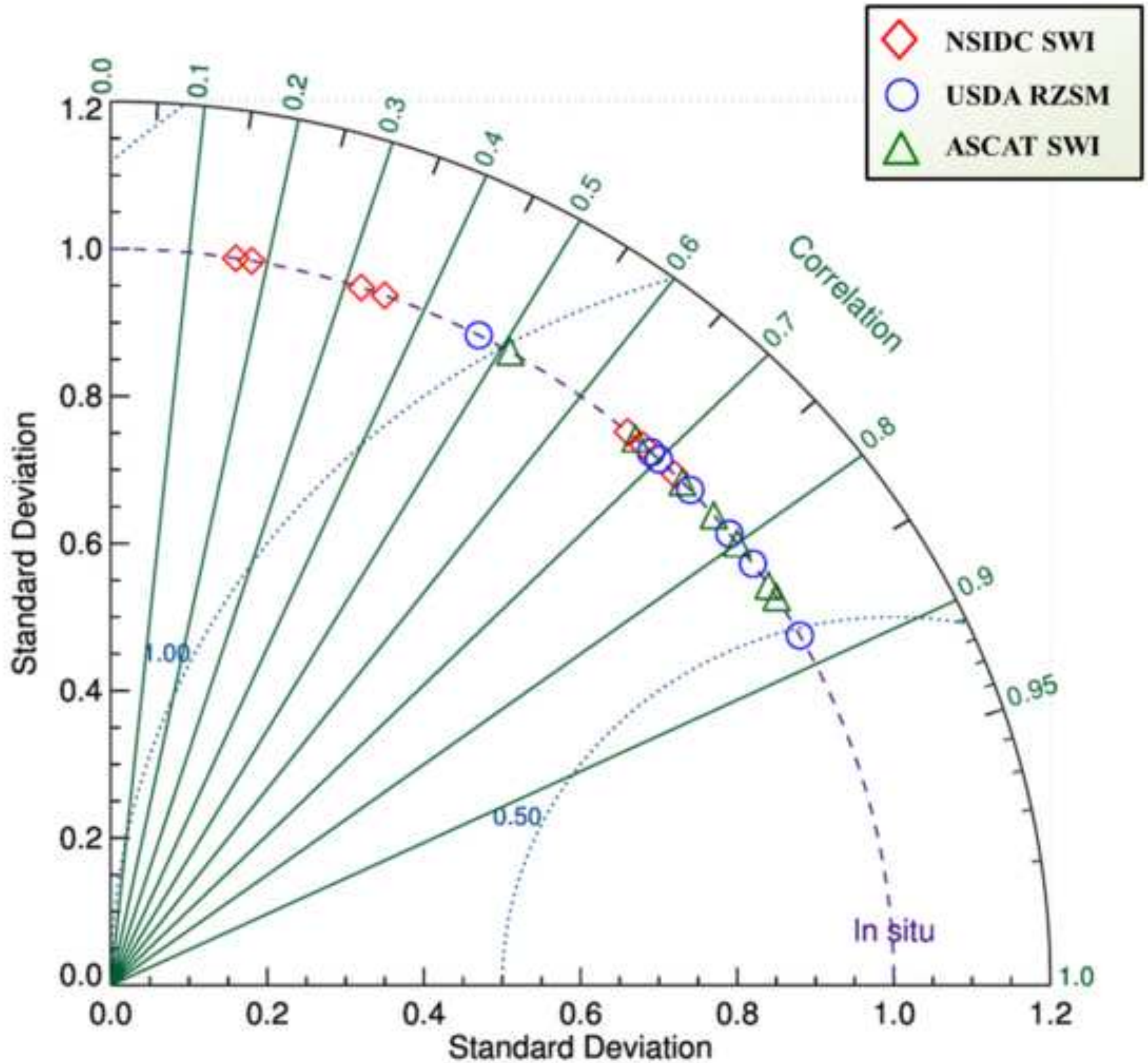

NSIDC SWI
USDA RZSM
ASCAT SWI
Correlation
0.0
0.1
0.2
0.3
0.4
0.5
0.6
0.7
0.8
0.9
0.95
1.0
Standard Deviation
1.2
1.0
0.8
0.6
0.4
0.2
0.0
1.00
0.50
In situ
0.0
0.2
0.4
0.6
0.8
1.0
1.2
Standard Deviation

Fig.6d

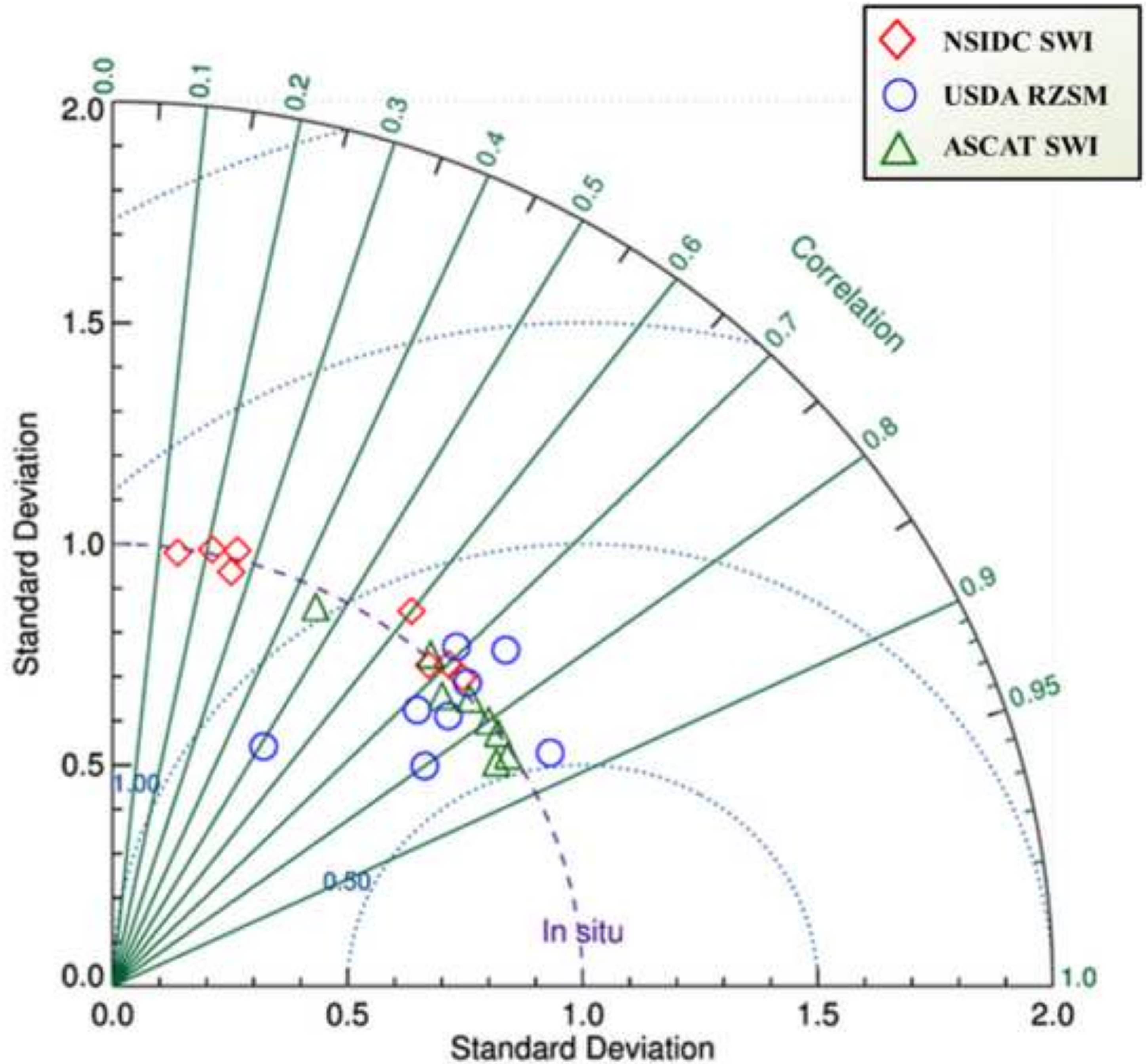

NSIDC SWI
USDA RZSM
ASCAT SWI
0.0
0.1
0.2
0.3
0.4
0.5
0.6
0.7
0.8
0.9
0.95
1.0
Correlation
Standard Deviation
2.0
1.5
1.0
0.5
0.0
Standard Deviation
1.00
0.50
In situ